



CHALMERS
UNIVERSITY OF TECHNOLOGY

Evaluation of the GIC module in PSS/E

Master of Science Thesis

LINUS KHOSRAVI

ERIK JOHANSSON

Evaluation of the GIC module in PSS/E

Master's Thesis in Electric Power Engineering programme

Linus Khosravi

Erik Johansson

Supervisor

Per Norberg, Energy and Environment, Division of Electrical Power
Engineering Chalmers University of Technology

Examiner

Anh Tuan Le, Energy and Environment, Division of Electric Power
Engineering Chalmers University of Technology

Abstract

Geomagnetic Induced Current (*GIC*) is a known threat to power systems. Previously there has been no commercial software available to simulate the stress this causes on the power systems. With the increased demand of investigating *GIC* scenarios *Siemens PTI* has developed a *GIC* simulation module within its software *PSS/E*.

This Master Thesis evaluates this *GIC* module. In order to perform simulations a fictive grid situated in the middle and south parts of Sweden was created with Oskarshamn as the main target of investigation. For this evaluation the student version of *PSS/E* was used which limited the power system to 50 buses. Therefore only the 400/135 kV transformers were evaluated together with the transformers from the generating units.

The simulations were performed for three different cases with three storm scenarios. The cases represented the transforming units in the early 90's and the upgraded transformer units for today with and without a grounding resistance at Oskarshamn. The storm scenarios evaluated had an electric field strength at 5, 10 and 20 V/km at a storm direction between $0 - 360^\circ$ stepped with 10° .

The results gathered from these simulations were compared with measured data to review the precision of the *GIC* module. From the simulations it was noted that the transformer types in the power system were subjected to the expected stress, that is that the reactive power losses at the transformers were highly dependent on the transformer core type. The simulated *GIC* at Oskarshamn differed from the measured peak value with 6%, however the precision in the resulting reactive power losses at each transformer type in the system could be questioned. That is because the *GIC* module uses a transformer model with a linear relationship between the subjected *GIC* and the reactive power loss. It is therefore recommended that the user, depending on the aim of precision, uses a more complex transformer model.

Acknowledgements

We would like to thank our supervisor Per Norberg at Vattenfall AB for his valuable guidance throughout the Master Thesis process and for motivating us in the subject of matter.

We would also like to thank Stefan Arnborg and Bertil Kielén at Svenska Kraftnät for their involvement in our project and giving us insight in their work on Geomagnetic Induced Currents. We would also like to express our gratitude towards Håkan Swahn at OKG AB for his helpful and interesting comments on the subject at hand.

Least but not last a special thanks goes to *Siemens PTI* for their support when using the software *PSS/E* and the *GIC* module.

Contents

1	Introduction	1
1.1	Aim	1
1.2	Objectives	2
1.3	Scope	2
2	<i>GIC</i> background	3
2.1	Solar storms	3
2.2	Geomagnetic storms	5
2.3	History	6
2.4	Solar storm measures	8
2.5	Conductivity	8
2.6	Transformer	10
2.6.1	Half cycle saturation	10
2.6.2	Increased even and odd harmonics	12
2.6.3	Flux heating	12
2.6.4	Transformer core type	12
2.7	Converting into a DC-model	13
2.7.1	2-winding transformers	14
2.7.2	Autotransformer	15
2.7.3	Transmission lines	15
2.7.4	Substation Ground Grid	16
2.8	Transformer reactive power	17
2.9	GIC module	19
2.9.1	GIC Outputs	24
2.9.2	GIC Output Files	24
3	Method	25
3.1	The power system	25
3.2	GIC Simulations	30
3.2.1	Simulation Prerequisites	30

3.2.2	Simulation Case	30
3.2.3	AC- vs DC-resistance	31
3.2.4	Power System Stability	31
4	Results	32
4.1	Simulations	32
4.2	Updated power system	36
4.2.1	Comparison of the changes between the two power system	39
4.2.2	Comparison between AC and DC branch data	41
4.2.3	Power system analysis	43
5	Discussion	45
6	Conclusion	47
	References	51
A	Appendix	52
A.1	400 KV Power System input data	52
A.2	135 KV Power System input data	55
A.3	GIC Data Input File	57
A.4	GIC Data Output File	59

1

Introduction

Geomagnetic Induced Current(*GIC*) is a major threat to the power systems, most noticeable for the power outage it caused in the region of Quebec in the late 1980's [1]. *GIC* occurs from differences in the geomagnetic field caused by solar storms. The storms alter the earth's magnetic field, a change in the magnetic field leads to an electric field. The transmission lines work as antennas for this electric field and will result in an induced voltage along the transmission lines. This voltage will create a current that travels along the transmission lines and closes a loop between two neutral groundings and the transmission line. This current is known as a Geomagnetic Induced Current(*GIC*).

As the frequency of the *GIC* is very low it can be considered as a DC current. This current causes half-cycle saturation of the transformer windings which will lead to hotspots, harmonic generation and increased reactive power absorption. Since the *GIC* behaves like a DC current protection relays treat them as zero sequence and can therefore trip.

The problems this has caused for the power systems, most noticeable in USA/Canada, has driven software manufactures to create modules for *GIC*. Therefore NERC (North American Electric Reliability Cooperation) has produced a manual on how to evaluate the impact of *GIC*. This new approach is used in the *PSS/E GIC* module and will be evaluated in this master thesis. The simulated values will be compared to real values provided by Vattenfall.

1.1 Aim

The aim of this master thesis is to evaluate the *PSS/E GIC* module and compare simulated results with acquired data from real *GIC* events in Sweden.

1.2 Objectives

During the project work various objects need to be finished to be able to solve the issues regarding the subject at matter and reach the aim of the project. The objectives are defined as the followings:

- Gather information about *GIC* effects on power systems

- Collect data for simulation in *PSS/E GIC* module

- Construct the DC-equivalent circuit for the *PSS/E GIC* module

- Compare the simulation results with *GIC* event data from Vattenfall

- Evaluate the *GIC* module and give recommendations regarding future work and the applicability of the module.

1.3 Scope

The simulations will be performed with parameters chosen in order to get the same induced current levels as observed by previously collected data. From the simulations, only the worst case scenario will be considered. All simulations will be done in steady state for a *DC – equivalent* circuit of the circuit scheme in order to simplify the model. The location of the simulation will be given as well as the cable length and design. The ground resistivity will be selected from values provided by Vattenfall and only a short description will be presented on how this is calculated. The power system will be limited and consists of the middle to south parts of Sweden.

2

GIC background

The Geomagnetic Induced Current (*GIC*) is a phenomenon that arises when charged particles are released from the sun and have the possibility to affect the power systems on the Earth. How the energy released from the Sun interacts with the Earth and hereby creates *GIC* and the effects that follows will be presented in this Chapter. It is also presented what is affected in the power system due to *GIC* and how the simulation software in *PSS/E* is used to simulate these effects.

2.1 Solar storms

The source to *GIC* is the energy the sun releases out into space referred to as the solar wind. The solar wind and how it occurs is therefore described in this section.

The sun is entirely gaseous and its outer layers which are of interest for solar storms are the following: the photosphere, the chromosphere and the corona. The photosphere consists of gases which are ionized and is the layer that is visible. The chromosphere lays between the photosphere and the corona and consists of hydrogen and is only visible during solar eclipse. The last and outer layer is the corona.

The solar wind is created in the corona layer where charged particles is continuously released outwards from the sun. For a solar storm to occur the solar wind created needs to carry a sufficient amount of energy. The extra energy injected into the solar wind comes from solar flares [2]. In Fig.2.1 the large eruptions on the sun sending out energy into the space can be seen.

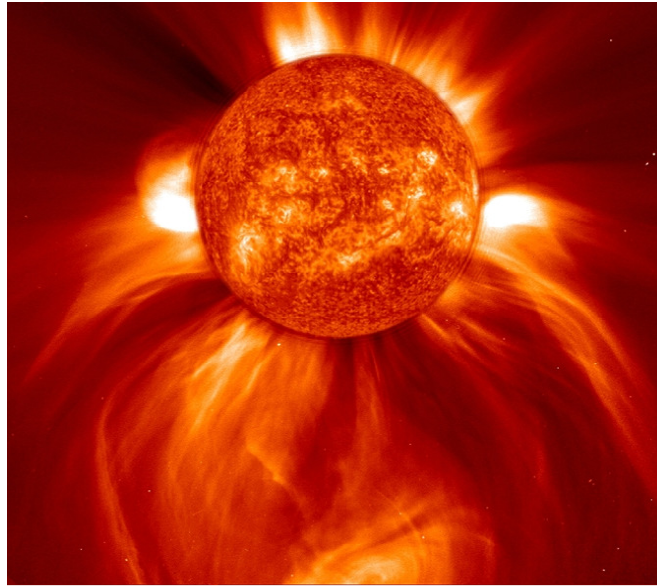


Figure 2.1: A picture showing energy eruptions on the sun [3]

Solar flares appear in the chromosphere. What solar flares do is that they convert stored magnetic energy into particle and electromagnetic emission. From which magnetic field arcs open in the corona layer which can create Coronal Mass Ejection (*CME*). When *CME* occurs it is possible that coronal matter is injected into the the solar wind. However, even if a solar flare creates *CME* a geomagnetic storm may not occur, only 20 % of the largest solar flares create geomagnetic storms.

Observations have shown that solar flares develop close to sunspots. The sunspots appear on the photosphere and have been studied since the 18th century. Fig.2.2 shows a picture of sunspots. From studying the sunspots it has been possible to estimate how often geomagnetic storms will occur because of their relation to solar flares. Geomagnetic storms occur with approximately a 11 year interval because that is the interval from where a sunspot disappears and later reappears [2].

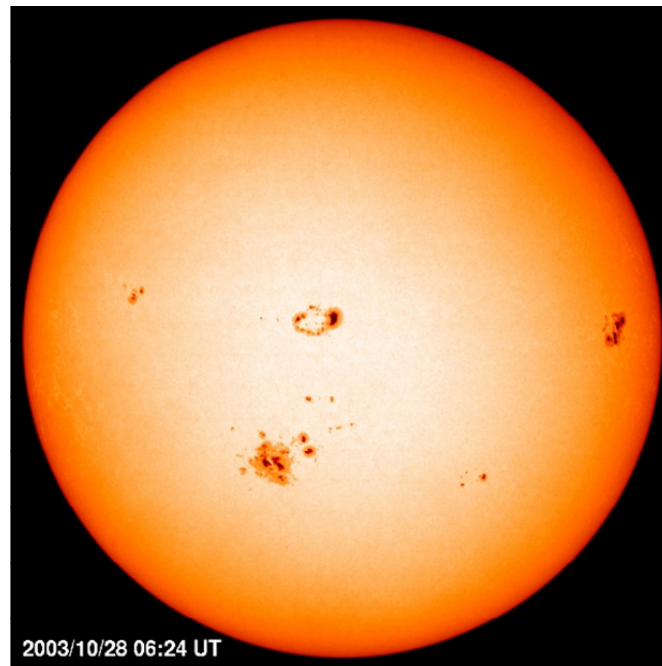


Figure 2.2: A picture taken showing sunspot appearance [4]

2.2 Geomagnetic storms

When the solar wind reaches the earth, i.e. the dayside, it interacts with the magnetic field of the earth. The solar wind, if it contains enough energy, compresses the magnetic field. This can go on from a few minutes up til several hours. When the magnetic field is compressed on the dayside it will expand on the nightside until it is long enough to break into two parts. The shape of the magnetic field, when it is compressed on the dayside and expanded on the nightside, is referred to as the magnetosphere. This can be seen in Fig.2.3. Due to the disconnection on the nightside, the collapse of the magnetosphere, large amounts of energy will flow into the poles of the earth. This event creates a current circling the poles at a height of 100 km with an amplitude up to $1\,000\,000\text{ A}$ [5] referred to as the electrojet. The electrojet creates a magnetic field which induces currents referred to as *GIC*. It is also the creator of auroras [6].

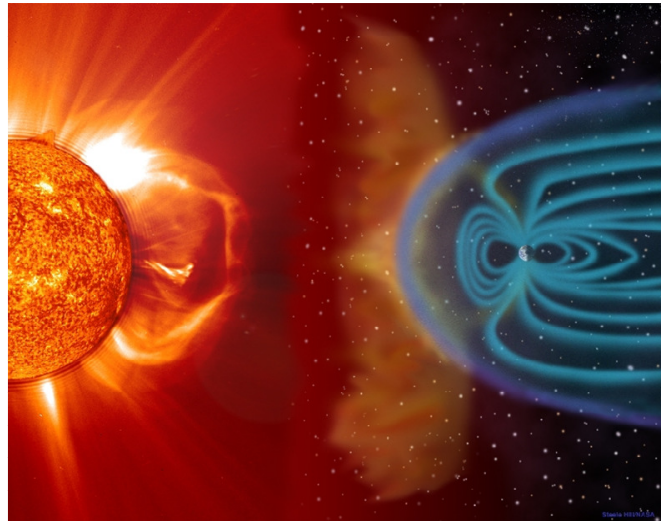


Figure 2.3: A picture of the sun and the solar storm sent into space affecting the magnetic field on earth [3]

It is also possible for solar winds to make the magnetosphere to collapse on the dayside of earth. For this to happen, it is required that the *CME* is very large. Another aspect is that solar winds do affect parts of the earth at lower latitudes. However the severity of these effects are less than than the effects closer to the poles but the duration will last longer which can cause harmful problems for power systems [7].

2.3 History

Several events over the years have shown what kind of impacts geomagnetic storms have had on the infrastructure. The most known storm occurred in 1989 causing a blackout in the province of Quebec, Canada. Other storms worth mentioning, causing issues are the Carrington event in 1859 which is named after the amateur astronomer by the name Richard Carrington who observed the solar activity leading to the events on earth [7] and the Halloween event in 2003 where solar storms in late September to early October affected electrical infrastructure in the southern parts of Sweden [1].

The difference in effects between the events regarding infrastructure and power utilities are greatest between the Carrington event and the more recent events. This is mainly due to the growth of electrical infrastructure.

The effect that was recognized by the storm in 1859 was mainly that the auroras that were created span over several continents which is an indication of the severity of the storm. The problems associated with the geomagnetic storm were mainly related to telegraph operating.

The geomagnetic storm that affected the earth in 1989 is mostly known for the power outage in the province of Quebec for approximately nine hours.

The reason to why the power outage happened was that the *GIC* flowing into the Hydro-Quebec power system made seven static compensators to shut down as they were damaged by the current, before any preventive measures could be taken. This led to further more disturbances in the power system and damaged equipment.

Sweden was also affected by the storm in 1989. For the central and southern parts of the Swedish power system, six 130 *kV* lines were disconnected.

A solar storm in 2003 led to disturbances not only in power systems but also for satellite communications as well as for the aviation industry. This is referred to as the Halloween event. Sweden and especially Sydkraft experienced problems during this event as transformers problems occurred leading to system failure and later power outage. Most of the problems that occurred was communication related, as airplanes and flight controllers had difficulties communicate with each other. There were also decisions made to reroute high latitude flights to suppress any effects on the communications issues. Also, in space, communication between earth and satellites were for some agencies down for some time and NASA issued preventive measures for the international space station such as no spacewalks.

From the historic events it can be concluded that geomagnetic storms can have severe effects on the world especially since the technical evolution has rapidly grown and increased the level of electrical solutions within the society. An effect of this is that costs related to geomagnetic storms can be very high. As an example if a storm of the magnitude of the Carrington event would occur today the cost estimation would be in the range of trillion dollars [1]. As also noticed over the time of history is that the power systems are vulnerable to geomagnetic storms which has a large impact of cost estimations for these kinds of problems. Issues related to geomagnetic storms are not only a concern to power systems but also communication as well as *GPS* systems. There are therefore three very important parts of society that can be severely affected related to geomagnetic storms. What then can be concluded from the report presented by *OECD*, is that the consequences related to *GIC* begins with problems affecting major basic necessities in society such as the power system, communications and positioning systems.

However it is important to acknowledge that severe or extreme storms are not very common as can be seen in Table 2.1 and that minor solar storms affect the earth all the time with only small effects such as reducing the life of transformers. The variation of the solar threat towards earth makes it very difficult to assess the level of preventive measures for these kinds of events [1].

Table 2.1: Geomagnetic storm (*DST*) level occurrence [8]

<i>DST</i> level [nT]	Occurance [frequency/years]
>100	4.6/year
>200	9.4/10 years
>400	9.73/100 years
>800	2.86/1000 years
>1600	7.41/1000000 years

2.4 Solar storm measures

There are different indexes for clarifying the the severity of solar storms. The indexes are Disturbance Storm Time index (*DST*), the *k* – index, the *G* – scale, the *a_k* – index and *db/dt* for changes in the magnetic field.

The *DST* index is an indicator of the intensity of the storm measured in nanoTesla (*nT*). The Carrington event is the worst storm ever to be measured and the *DST* level was -1760 *nT*. This can be compared to the event causing the blackout in Quebec which had a measured level at -640 *nT*. A severe storm is described to have a *DST* level of less than -500 *nT* which shows that these two events mentioned earlier were severe. In comparison, the Halloween event in 2003 only reached a *DST* level of -410 *nT* [1].

The *k* – index has a range between 0 – 9 and is a index of the change in the magnetic field of the earth during a 3-hour period. A severe storm is in the range of 7 – 9 whilst a minor storm has the level 5.

The *a_k* index however ranges from 0 – 400 and is based on the magnetic field changes over a 24 – hour basis derived from the *k* – index over eight days. For a severe storm the range is between 100 – 400 whilst for a minor storm the range is between 30 – 50.

The *G* – scale is based on the *k* – index and has level 1 – 5 declaring the severity of the storm, where level 5 is the worst scenario [1].

For power system operators it is however most common to use *db/dt* to establish the changes in the magnetic field. This is due to that the impact on power systems can go on for only seconds or minutes. It therefore gives a more accurate view on the effects as *db/dt* can show higher peak values than the other indices [7].

2.5 Conductivity

A main part of the contribution to the severity of *GIC* is the ground conductivity. This is due to its effect in the relationship between the geoelectric field and the geomagnetic

field which is described in eq.2.1

$$E(\omega) = Z(\omega) \cdot H(\omega) \quad (2.1)$$

Here $E(\omega)$ represents the geoelectric field in V/m , $Z(\omega)$ is the surface impedance in Ω and $H(\omega)$ is the geomagnetic field intensity in A/m .

As the conductivity differs depending on location the impact of geomagnetic disturbances also differs. To be able to determine the conductivity of locations the impedance of the ground needs to be investigated.

The simplest way to obtain the surface impedance, to be able to find out the effects on the magnetic field due to *GIC*, is to use a 1 – *D*-model of the earth and its layers. The 1 – *D*-model is based on transmission line theory which means that the problem is dealt with in the manner of reflection between the layers of the earth. The deepest layer of the earth has no reflection and is having the propagation coefficient infinite whilst the other layers have different propagation coefficients. The calculation strategy used is starting with the deepest layer calculating each outer layer until the surface is reached [9].

The propagation constant for a layer is described by the following equation:

$$k_n = \sqrt{j\omega\mu_0\sigma_n} \quad (2.2)$$

Here ω represents the angular frequency in *radians/second*, μ_0 is the magnetic permeability of free space and σ_n is the conductivity in $(\Omega m)^{-1}$ for the layer n . The surface impedance is characterized by the following equation for the bottom layer:

$$Z_n = \frac{j\omega\mu_0}{k_n} \quad (2.3)$$

The reflection coefficient r_n for layer n seen by the layer above is calculated as follows:

$$r_n = \frac{1 - k_n \frac{Z_{n+1}}{j\omega\mu_0}}{1 + k_n \frac{Z_{n+1}}{j\omega\mu_0}} \quad (2.4)$$

This is used to calculate the impedance on the top surface of layer n which is as follows:

$$Z_n = j \cdot \omega \cdot \mu_0 \left(\frac{1 - r_n \cdot e^{-2k_n d_n}}{k_n (1 + r_n \cdot e^{-2k_n d_n})} \right) \quad (2.5)$$

where d_n is the thickness of the layer n in meters. These steps are repeated for every layer until the surface layer is reached.

Furthermore, contrasts in areas, geographically, such as coastal lines, present other issues to the conductivity problem. The issue at hand is that the conductivity is higher at the sea compared to the land, therefore the current flowing in the sea is higher than the current flowing in the land. The boundary between land and sea creates an inequality.

As the boundary can not accumulate charge, the inequality creates a potential gradient that equalises the current magnitude between sea and land. This makes the current higher at land and lower at sea. For these contrasts it is recommended to use a 2 – D - or a 3 – D -model to obtain more accurate results. [9] It should however be mentioned that the surface conductivity data is most often gathered from geological institutes or measured at a given location.

2.6 Transformer

The main area of concern regarding *GIC* is the large power transformers. Power transformers today have been optimized to the level of only requiring a few amperes of exciting current in order to produce the necessary magnetic flux for the voltage transformation. Therefore problems arise during a *GIC* event that can induce quasi DC current that may exceed up to 20 times the peak value of the magnetising current [10].

There are three main areas that affect the power transformer during an *GIC* event:

1. Increased reactive power consumption
2. Increased even and odd harmonics
3. Stray flux heating causing hotspots

2.6.1 Half cycle saturation

Transformers use iron cores in order to reduce the reluctance of the flux path. This is desired in order to keep the circulating current as low as possible. However, by using an iron core non-linearity is introduced into its operation. The transformers are designed to utilize the linear range of the iron core with small non linear operations during voltage peaks. This results in a small excitation current. However when a power transformer is subjected to a DC current, as in a *GIC* event, the DC current creates a flux offset. This is illustrated in Fig.2.4. The DC flux adds to the AC flux in half a period and subtracts in the other. This causes the transformer to operate in the non-linear range of the transformer core leading to saturation for a half cycle. When the transformer operates with a saturated core it causes it to draw a large asymmetrical exciting current full of even and odd harmonics[11].

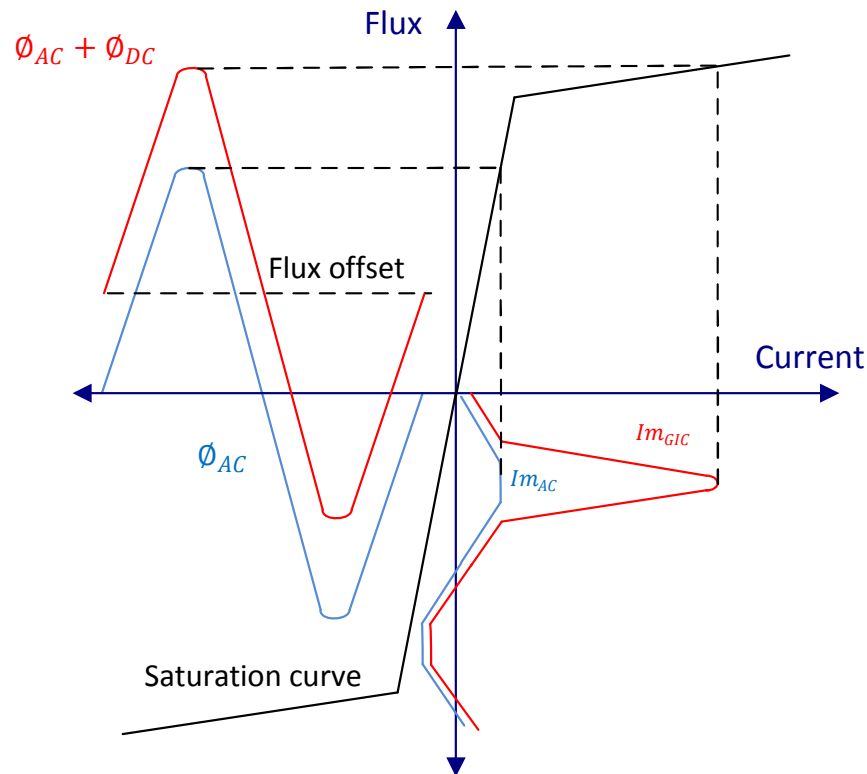


Figure 2.4: Half-Cycle Saturation [11]

Since the excitation current is purely reactive (lags the system voltage by 90°) this results in an increase in reactive power loss. A test made on a 3 phase bank of single phase 500/230 kV transformers by [12] showed an increase in reactive power loss from 1 MVar during normal operation to 40 MVar during an GIC event with 25 A induced in each phase. Since a geomagnetic storm effects large parts of the power system simultaneously, the increased demand in reactive power from the transformers can be overwhelming and in worst case lead to a voltage collapse. From the GIC event in Quebec 1989 measurements showed an increase in reactive power of 420 MVar from a single substation. It should be noted that depending on the design of the core the impact of the induced currents differ. For instance, the 3-phase 3-legged core-form transformer has shown to be less susceptible to induced current. Therefore when performing analysis of the impact of GIC it is important to take into account the different kinds of transformers in the power system [13].

2.6.2 Increased even and odd harmonics

The even and odd harmonics produced by the increased and distorted excitation current creates problem for the other apparatus in the power system. Specifically the protection relays where they can cause unwanted operation [14]. The harmonics usually includes the first 10 orders with varying levels depending on the *GIC*. However a large *GIC* may result in lower Total Harmonic Distortion (*THD*) since the transformer consumes more of the fundamental frequency current [15].

2.6.3 Flux heating

With a saturated core the flux will no longer be contained within the transformer. Instead the flux will travel through adjacent paths which might involve the transformer tank or core clamping structures. This stray flux will induce eddy currents that is converted to heat. Since a *GIC* event can last for hours this can severely damage the transformer. These hotspots have been noted to damage the paper winding insulation, create impurities in the insulation oil and so on [16].

2.6.4 Transformer core type

There are two main types of transformer core designs to consider, the shell and the core type. The core design uses cylindrical windings wrapped around the legs of the core with the Low Voltage (*LV*) windings inside the High Voltage (*HV*) windings. The shell type however encloses its core around the windings with the *HV* and *LV* windings stacked side by side in an oval shape. Both these designs have advantages and disadvantages. The shell type is more cost effective as the core can be adjusted around the coils in an optimal way. However the core design offers beneficial characteristics for large power transformers as they can handle the short circuit forces better.

The different transformer core types are susceptible to *GIC* unequally. This is due to the design of the different core types. The design of the core type will affect the path of the traveling flux generated by the *GIC*. This flux is often referred to as DC-flux but the name zero-sequence-flux is a more suitable word for understanding the event with *GIC* [17]. The zero-sequence-flux generated by the *GIC* needs a closed path to travel. Depending on the design of the transformer this path is different. If the design requires the zero-sequence-flux to travel outside the core, it will not create saturation that easily. This is because the reluctance outside the core is much higher, decreasing the effect of the zero-sequence-flux. Therefore a higher current is needed for those transformer designs to saturate as flux and current correlate [18].

The only transformer design that offers the zero-sequence-flux to travel outside the core is the 3-phase 3-leg core type. This means that this design is preferable regarding *GIC* disturbances. The zero-sequence-flux for the different transformer design can be

seen in Fig. 2.5. The zero-sequence-flux path for the 3-phase 3-leg core can be represented by Fig.2.5b. Compared to the other transformers no small arrows representing how the zero-sequence-flux travels in the cores are shown as the flux path travels outside the core. It can be seen from Fig.2.5a and Fig.2.5d that single phase and 3-phase 5-leg core type are somewhat comparable regarding the paths for the zero-sequence-flux. However it should be noted that single phase transformers are the most susceptible design for *GIC* disturbances. The different transformer designs could be listed as the following regarding the susceptibility of half-cycle saturation [19].

1. 3-phase 3-leg core
2. 3-phase 5-leg core
3. 3-phase shell/conventional
4. 3-phase shell/7-leg core
5. Single phase shell/core

The following figures shows the DC-flux in different core types and designs:

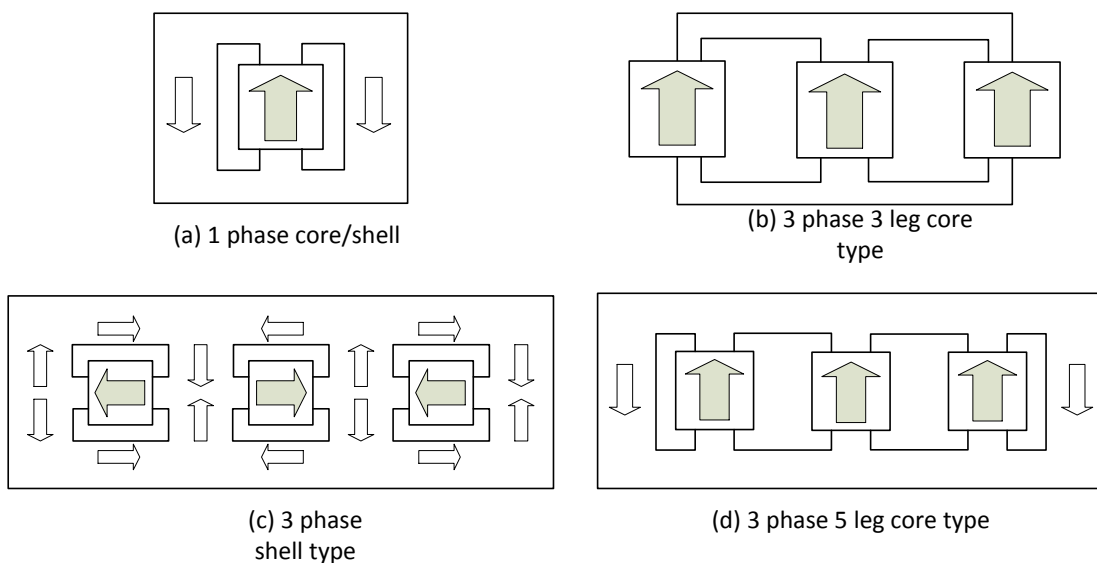


Figure 2.5: DC flux path for transformer cores [20]

2.7 Converting into a DC-model

Since the *GIC* are of low frequency they can be considered as a DC. Therefore a DC model of the network must be performed. This section will present the parameters to be considered when performing such an analysis on a power system.

2.7.1 2-winding transformers

When constructing a DC-model of a 2-winding power transformer, only paths that have a physical connection to ground are considered. Therefore mutual coupling and windings where no such connection exist are excluded. This also applies for 3-winding transformers as the tertiary winding provides no path to ground for the *GIC* to flow. The same logic is applied for delta connected windings. The transformation of a 2-winding transformer into an equivalent DC circuit is demonstrated in 2.6. The DC resistance values for the HV windings, $R_{w1}/3$, and the LV windings, $R_{w2}/3$, should be taken from transformer test reports if available. The neutral points (X_0 and H_0) are connected to the substation ground or in some cases left floating. It is at these nodes, X_0 and H_0 , that *GIC* blocking devices should be implemented. If the option is available to implement a *GIC* blocking device directly, then only the resistive value needs to be entered. Otherwise, since it is in series with the winding resistance, the resistive value of the blocking device can simply be added to the series resistance [21]. The effects of implementing a blocking device is highly dependent on the size of the device. For implementation of a blocking resistance the value of the resistance may affect the operations of the transformer as well as the protection relays. However for small resistances the impact on the transformers zero sequence network is small and there often is no need to reconfigure the system. But with increased size problems arise. The transformers protection relays needs to be reevaluated as well as the transformers connection to ground in order to avoid overvoltages [22]. For this Master Thesis the impacts of blocking devices will only regard the transformers and not the power system as this is not within in the scope of investigation.

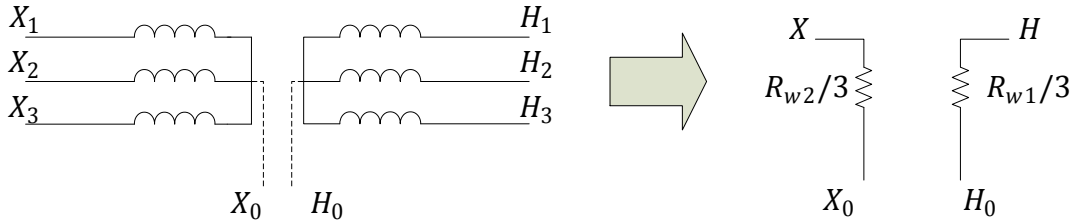


Figure 2.6: 2-winding power transformer converted into a DC-model

If the series winding resistance is not available and some error is acceptable they can be estimated. This is done by taking the positive sequence resistive data, R_{ps} from power flow and short circuit analysis.

$$R_{ps} = \frac{R_{w1} + n^2 R_{w2}}{Z_{bh}} \quad (2.6)$$

where Z_{bh} is the high voltage base impedance and n is the turn ratio. The assumption then needs to be made that the high voltage and medium voltage winding resistance is equal and that the turn ratio $n = 1$. From this the high voltage winding resistance can

be calculated as:

$$R_{w1} = \frac{1}{2} \cdot R_{ps} \cdot Z_{bh} \quad (2.7)$$

2.7.2 Autotransformer

The autotransformer is not particularly different from the 2-winding transformer and the 3-winding transformer when constructing its DC-model. This can be seen in Fig.2.7.

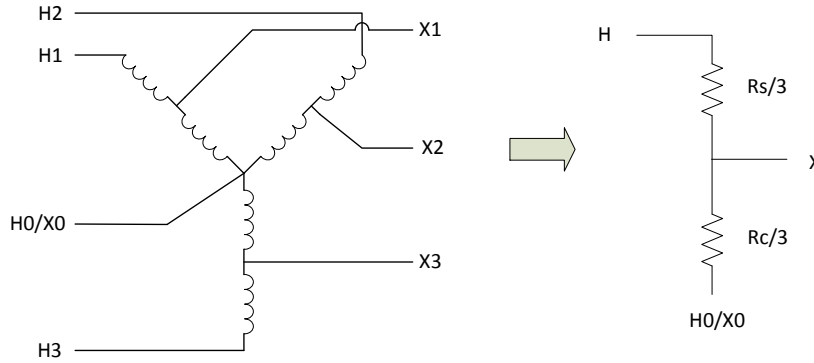


Figure 2.7: Autotransformer converted into a DC-model [23]

The windings present in the model is represented by resistance for the series winding, $R_s/3$ and the common winding, $R_c/3$. Where R_s and R_c are the DC-resistance values for the windings. As for the 2-winding transformers and the 3-winding transformers the resistance values, if not available, can be calculated using power flow short circuit analysis as:

$$R_s = \frac{1}{2} \cdot R_{HX} \cdot Z_{bh} \quad (2.8)$$

Here R_{HX} is the per unit positive sequence resistance and Z_{bh} is high voltage base impedance.

$$R_c = \frac{1}{2} \cdot \frac{R_{HX} \cdot Z_{bh}}{(n-1)^2} \quad (2.9)$$

Where n is the voltage ratio between line to ground for the H and X nodes [23].

2.7.3 Transmission lines

The variations of the geomagnetic field, $\frac{\partial B}{\partial t}$, leads to an induced electric field. By integrating the electric field along the transmission line the induced voltage can be calculated as:

$$V_{dc} = \oint \vec{E} \circ d\vec{l} \quad (2.10)$$

where \vec{E} is the electric field vector and $d\vec{l}$ is the incremental line segment including direction between two substations. If the electric field is assumed to be constant along the transmission line only the coordinates of the substations need to be taken into account. Thus the line segment $d\vec{l}$ becomes \vec{L} . Both \vec{E} and \vec{L} can be divided into x and y coordinates and the induced voltage can therefore be calculated as:

$$V_{dc} = \vec{E} \circ \vec{L} = E_x L_x + E_y L_y \tag{2.11}$$

where x denotes the field and length in northward direction and y in eastward direction. As the earth is shaped as an ellipsoid the lengths, L_x and L_y , will depend on the earth model used. *PSS/E* uses the WGS84 model which is the model used in the GPS system.

The resistive component of a transmission line should be selected at a temperature of 50° to simulate a loaded network. However if no such information is available it is acceptable to apply the AC resistive value extracted from power flow simulations. Depending on the diameter of the conductor this introduces marginal errors. However at a conductor diameter of up to 1.25 inch this error is only 5%. In Fig.2.8a single phase DC schematic of a conductor is presented. Here the DC voltage source is the geoelectric magnetic field and R_{DC} is the total DC resistance of the 3-phase conductor including bundling effects [24].



Figure 2.8: One phase DC schematic of a conductor

2.7.4 Substation Ground Grid

When considering the DC-equivalent resistance of the substation ground, parameters as shield wires and multi-grounded neutral conductors need to be taken into account. All transformers in the substation are connected to the same ground and therefore only one value for the substation ground is needed. This is illustrated in Fig.2.9 where R_{gnd} is substation ground resistance and R_b are the transformer *GIC* blocking devices. The most common way of estimating R_{gnd} is by using the value obtained from the fundamental AC frequency resistance [25].

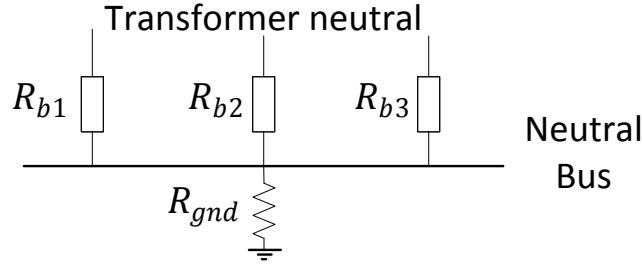


Figure 2.9: DC schematic of a Substation

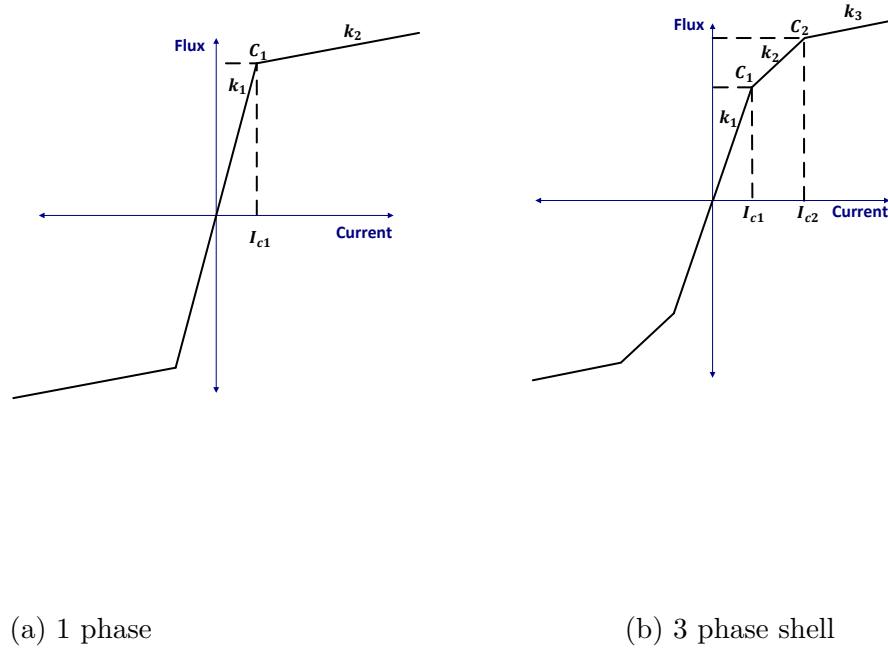
2.8 Transformer reactive power

In order to be able to calculate the reactive power loss in transformers a simplified method is used in *PSS/E*. This method relies on the *GIC* and nameplate information of the transformers as inputs in order to estimate the reactive power loss. This method however does not take into account any iron or copper losses and the leakage flux is ignored for all types except for the 3-phase 3-legged core type transformers.

The reactive power loss is defined as:

$$Q = 3 \cdot U_1 \cdot I_1 \quad (2.12)$$

Where U_1 is the RMS value of $u(t)$ and I_1 is the fundamental component of $i(t)$. In order to be able to estimate the harmonic currents the magnetization curve of the transformer must be known. To determine the magnetization curve of a typical transformer a piecewise linear representation can be used. For the single phase transformers the magnetization curve can be represented by three straight lines, independent of core type, as it only has one common main flux path, this is illustrated in Fig. 2.10a. Here k_1 is the slope of the line and the current I_{c1} at the knee C_1 is commonly referred to as $1.1 \cdot \sqrt{2} \cdot I_{RMS}$ where I_{RMS} is the *RMS* value of the normal exciting current. For the three phase transformers the core must be taken into account. The reason for this is that the AC and DC flux paths are different for different cores as mentioned in Section.2.6.4. In Fig.2.10b the piecewise linear representation of a 3-phase shell type transformer is illustrated. The model is defined by five lines where k_1 and C_1 can be determined from the rated voltage and the normal exciting current. The slope k_2 , k_3 and the knee C_2 must be determined by field studies [26].



(a) 1 phase

(b) 3 phase shell

Figure 2.10: Linear piecewise representation

If the *GIC* is large enough, more than five times the exciting current, the normal exciting current can be ignored. Simulations done on the exciting current in [26] show a linear increase on the fundamental component with an increase of *GIC*. Therefore a linear relation between the reactive power loss and *GIC* can be estimated by calculating Eq.2.12 and determining the slope. An estimate for the *MVar* consumption of the different types of transformers can then be estimated by:

$$Q(MVar) = k \cdot GIC + Q_0 \quad (2.13)$$

Where k is the slope determined from Eq.2.12 and Q_0 is the reactive power consumption from the normal exciting current. Values for the slope k for different core types is given in Table 2.2[26].

Table 2.2: k-factor for different core designs

Core design	k
Single phase	1.18
Three phase shell form	0.33
Three phase 3 legged core form	0.29
Three phase 5 legged core form	0.66

2.9 GIC module

The *GIC* analysis tool in *PSS/E* is part of the power flow analysis that can be performed in the program. The module offers the user to simulate a storm creating an electric field with a determined direction. From the module it is possible to determine reactive power losses in the system and the currents that are created. It is also possible to use information gathered by simulation and use it for power flow simulations in *PSS/E*. The basis used for the calculations performed in the *GIC* module are explained in Section.2.7. As explained, a DC-model need to be constructed and for the units in the power system DC values need to be determined.

The module itself is visual based which means that everything regarding the *GIC* data is run by the the *GIC* analysis window. The *GIC* analysis window can be seen in Fig.2.11. From this window the input parameters are set for each simulation. The inputs for the simulations are storm direction and electric field strength. The storm direction is given by an angle, (0 – 360°) whilst the electric field strength is given in the unit *V/km* or *V/mile*. In this window it is also decided which outputs are desired for the simulation.

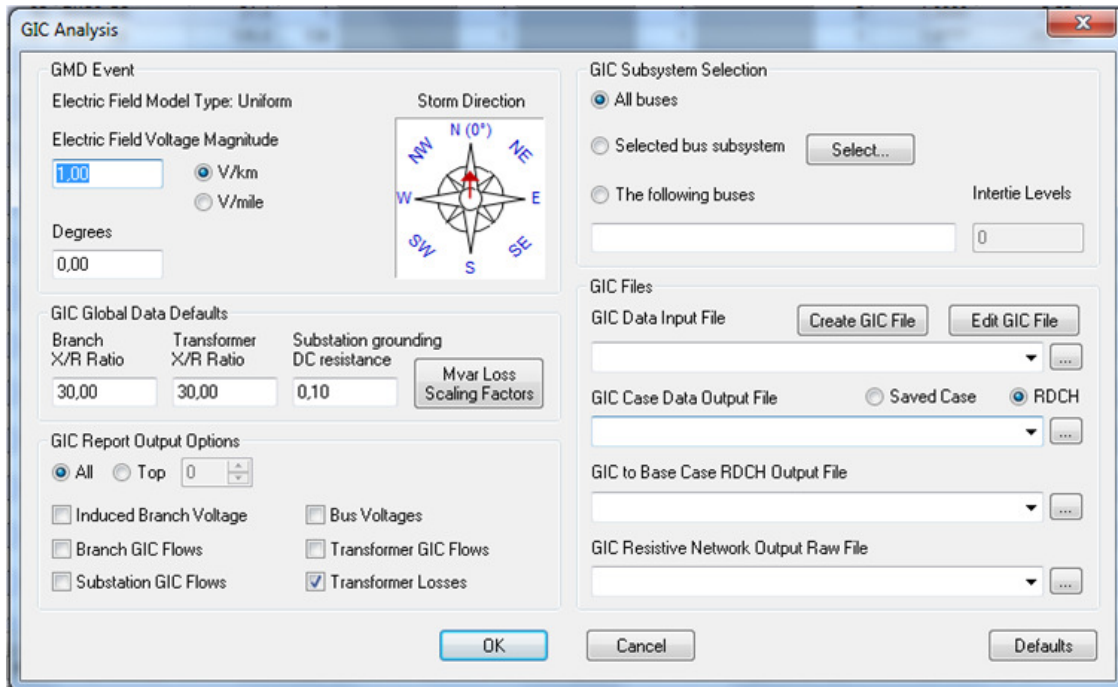


Figure 2.11: GIC analysis window

To be able to perform any simulations, a *GIC* file need to be created. This file need to contain information about the substations, the buses and the transformers in the system. The user creates the file in the *GIC* window. The *GIC Input Data File* can be seen in A.3. It should be noted that the *GIC* analysis tool collaborates with the system created in *PSS/E* which means that the created file is based on the prerequisites of the system.

The *GIC* window have three tabs, substations, buses and transformers. As can be seen in Fig.2.12 which shows the tab for substations, this data need to be filled in manually in accordance to the power system. The data required consists of number, name, geophysical location in degrees, longitude, latitude and DC grounding resistance in ohm [27].

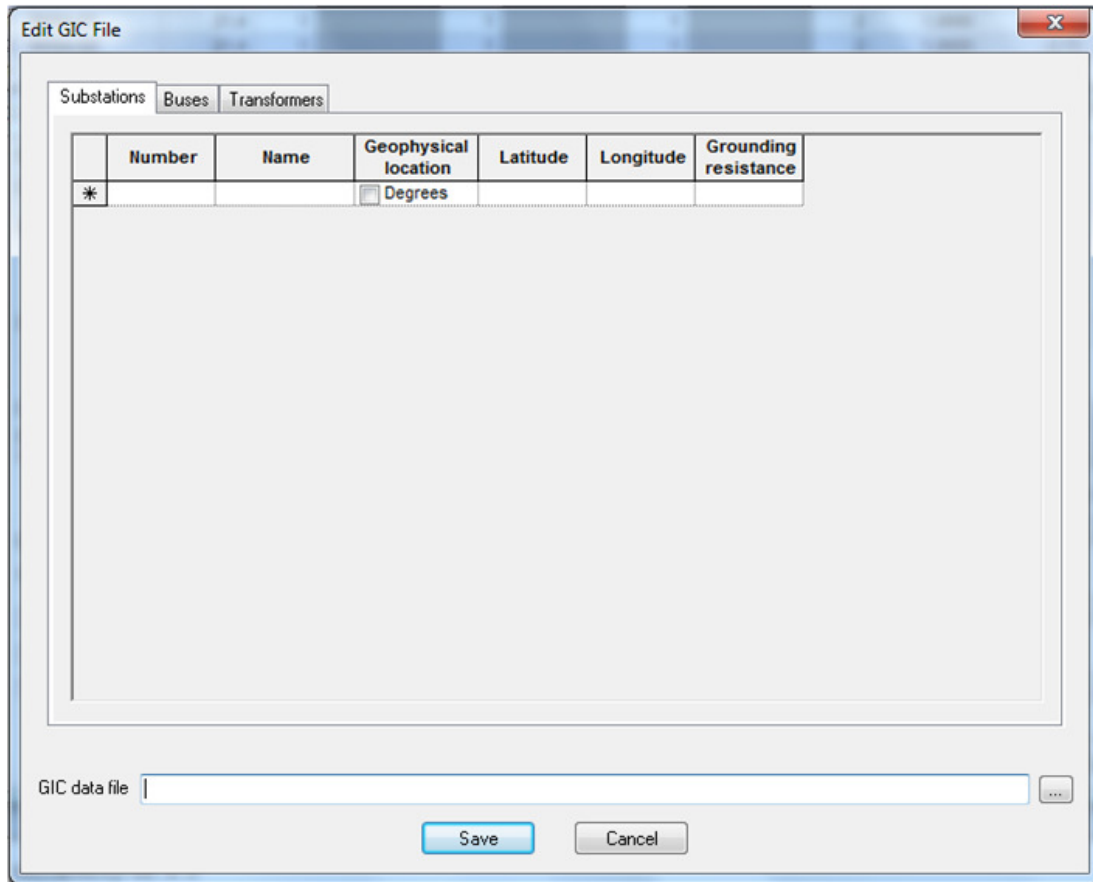


Figure 2.12: Substation data tab

The tab, buses, show all the buses that are in the power system, as can be seen in Fig. 2.13.

Number	Name	Substation number
1	O2-G	21,300
2	O3-G	20,500
11	RHS4-G1	21,4
12	RHS4-G2	21,4
91	RHS3-G1	21,4
92	RHS3-G2	21,4
101	SVP-130	135,
103	NKP-130	135,0
104	LKP-130	135,0
106	SKD-130	135,
107	GBG-130	135,
110	RHS3-130	135,
111	TRA-130	135,
112	JKP-130	135,0
113	AVA-130	135,
114	KHM-130	135,
205	HAG-200	220,
401	SVP-O2	400,0
402	SVP-O3	400,0
403	NKP-400	400,0
404	LKP-400	400,0

Figure 2.13: Bus data tab

The transformer tab shows the transformers in the power system and consists of data already determined in the power system file and additional transformer data that needs to be typed in manually. The transformer tab shows every transformer connected between two buses. The option of blocking resistor is also present and is zero by default. Activating the blocking resistor will stop the *GIC* to flow in the transformer neutral. The winding resistance is referred to as from bus resistance (HV) and to bus resistance (LV). The vector group is collected from the case file for the power system created. The core for each transformer need to be set manually and it is possible to choose from, single phase, 3-phase 3-leg, 3-phase 5-leg, 3-phase shell and unknown which is set as default. The last step is the option to set the k – factor which is 0.000 by default. The transformer tab can be seen in Fig.2.14.

Id	From bus resistance	To bus resistance	Last bus resistance	Vector Group	Cores	K Factor
1	2,971	2,971	0,000	YNd1	Unknown	0,000
1	0,101	0,101	0,000	YNd1	Unknown	0,000
1	0,348	0,348	0,000	YNd1	Unknown	0,000
1	0,348	0,348	0,000	YNd1	Unknown	0,000
1	0,355	0,355	0,000	YNd1	Unknown	0,000
1	0,354	0,354	0,000	YNd1	Unknown	0,000
1	0,261	0,261	0,000	YNd0	Unknown	0,000
1	0,196	0,196	0,000	YNd0	Unknown	0,000
1	0,167	0,167	0,000	YNd0	Unknown	0,000
1	0,164	0,164	0,000	YNd0	Unknown	0,000
1	0,338	0,338	0,000	YNd0	Unknown	0,000
1	0,261	0,261	0,000	YNd0	Unknown	0,000
1	0,266	0,266	0,000	YNd0	Unknown	0,000
1	0,170	0,170	0,000	YNd0	Unknown	0,000
1	0,261	0,261	0,000	YNd0	Unknown	0,000
1	0,198	0,198	0,000	YNd0	Unknown	0,000
1	0,131	0,131	0,000	YNd0	Unknown	0,000
*						

Figure 2.14: Transformer data tab

If the k -factor is set to default the simulations in the *GIC* module will be performed with k -factor values determined by the *Mvar scaling factors*. Here each transformer core has a predefined k -factor for calculations. However this requires that the core type of each transformer in the system are defined in the *GIC* file. The equation used for reactive power losses with a default k -factor is:

$$Mvar\ loss = k * I_{GIC} * \left(\frac{kV_{highwinding}}{kV_{specified}} \right) \quad (2.14)$$

Here the $kV_{highwinding}$ is the nominal voltage level for the transformer specified in the system file whilst the $kV_{specified}$ is determined by the user.

If the k -factor is defined the equation for the reactive power losses is as follows:

$$Mvar\ loss = k * I_{GIC} \quad (2.15)$$

2.9.1 GIC Outputs

The outputs generated by the *GIC* module are, *Induced Branch Voltage*, *Branch GIC Flows*, *Substation GIC Flows*, *Bus Voltages*, *Transformer GIC Flows* and *Transformers Losses*. It is also a possibility to select if all buses, some buses or a subsystem should be simulated. For *Transformer losses*, the output data consists of reactive power losses in the windings, separating the different winding transformers and auto transformers. The data also shows the total amount of reactive power losses in the system. It should also be noted that the reactive power losses for the transformers are summarized for the different winding transformers and auto transformers in all outputs.

The data output for *Induced Branch Voltage* contains information about the voltage and the current that are induced on the branches as well as the closest distance between the buses.

Branch GIC Flows shows the current flowing in the branches with no transformer connection and also calculates the closest path between the buses.

For the *Substation GIC Flows* the data generated consists of the current flowing from ground substation. *Bus Voltages* shows the bus and substation ground bus DC voltage. *Transformer GIC Flows* shows the current flowing in the windings for the different transformers [27].

2.9.2 GIC Output Files

There are three different output files that can be generated to be able to do other simulations in *PSS/E* using the data from the *GIC* simulation. *GIC Data Case Output File* which can be saved as a saved case file or a *RDCH* (Read Change), *GIC to Base Case RDCH Output File* and *GIC Resistive Network Output Raw File*. The *GIC Data Case Output File* is used for power flow solutions where the reactive power losses in the transformers are converted to constant current loads. The file can be seen in A.4. The *GIC to Base Case RDCH Output File* creates a *RDCH* file containing the reactive power losses loads for transformers which have shutdown. The *GIC Resistive Network Output Raw File* transforms the power flow network into a resistive network for *GIC* calculations. It should however be noted that the number of buses will be increased due to grounding resistance for substations and transformer winding connections [27].

3

Method

As the analysis is based on the student version of *PSS/E* the simulations are limited to a 50 bus system. Historically the problems with *GIC* has arisen in the south of Sweden. Therefore the analysis of the *GIC* module is based on a fictive power system illustrating the mid and southern parts of Sweden. The northern part is excluded since the impact of *GIC* less noticeable.

3.1 The power system

In order to represent the 400 kV system for the middle to southern parts of Sweden 14 nodes were selected. The main focus of these nodes was to represent the system accurately where known problems have arisen due to *GIC*. The more substations that are included in a area the more accurate results will be obtained. Since the evaluation is limited to a 50 bus system simplifications has to be made. Explicitly one main area has had documented interference and installed improvements in the previous decades. This area is Oskarshamn 3. Therefore Oskarshamn was chosen to be the main interest of this evaluation and as many substations as possible in the near vicinity of Oskarshamn was included to get as accurate results as possible. Gothenburg and Jönköping will also be analyzed as their transformers have been updated but both are represented by a single substation. As the impact of *GIC* is largest for the high voltage system the low voltage system will be neglected. The complete list of substations in the 400 kV grid based on public data and estimated positions is listed in Table A.1 as well as their ground resistivity.

The geographical position of the substations as well as the DC grounding resistance is the next step in determining the interconnections between the substations as well as the cable type and its equivalent DC resistance. Since this power system is based on the actual power system of Sweden the real interconnections between these substations

exists. In Table.A.2 the connections are given as well as cable type, length and their impedance properties based on public data.

There are two power plants supplying the 400 kV grid, Ringhals in the west and Oskarshamn in the east. Ringhals is represented by four generating units and Oskarshamn by two. These are presented in Table A.3 where O3-G is selected as the slack bus.

The complete model for the 400 kV system can be seen in Fig.3.1. The last step and the most important for determining the impact of the *GIC* is the transformers. The transformers in question are both transformers for the generating units as well as the 400/135 kV transformers. As mention in Section.2.6 a number of properties needs to be extracted for the transformers in use. Most notably is the transformer core design and its high and low voltage series winding DC resistance. The actual transformer data at these substations was acquired and is presented in Table.A.4. Since the delta connections offer no paths to ground their resistive values are not relevant and are therefore presented by a $-$. The k – *factor* is the default factor that *PSS/E* uses for different transformer core designs.

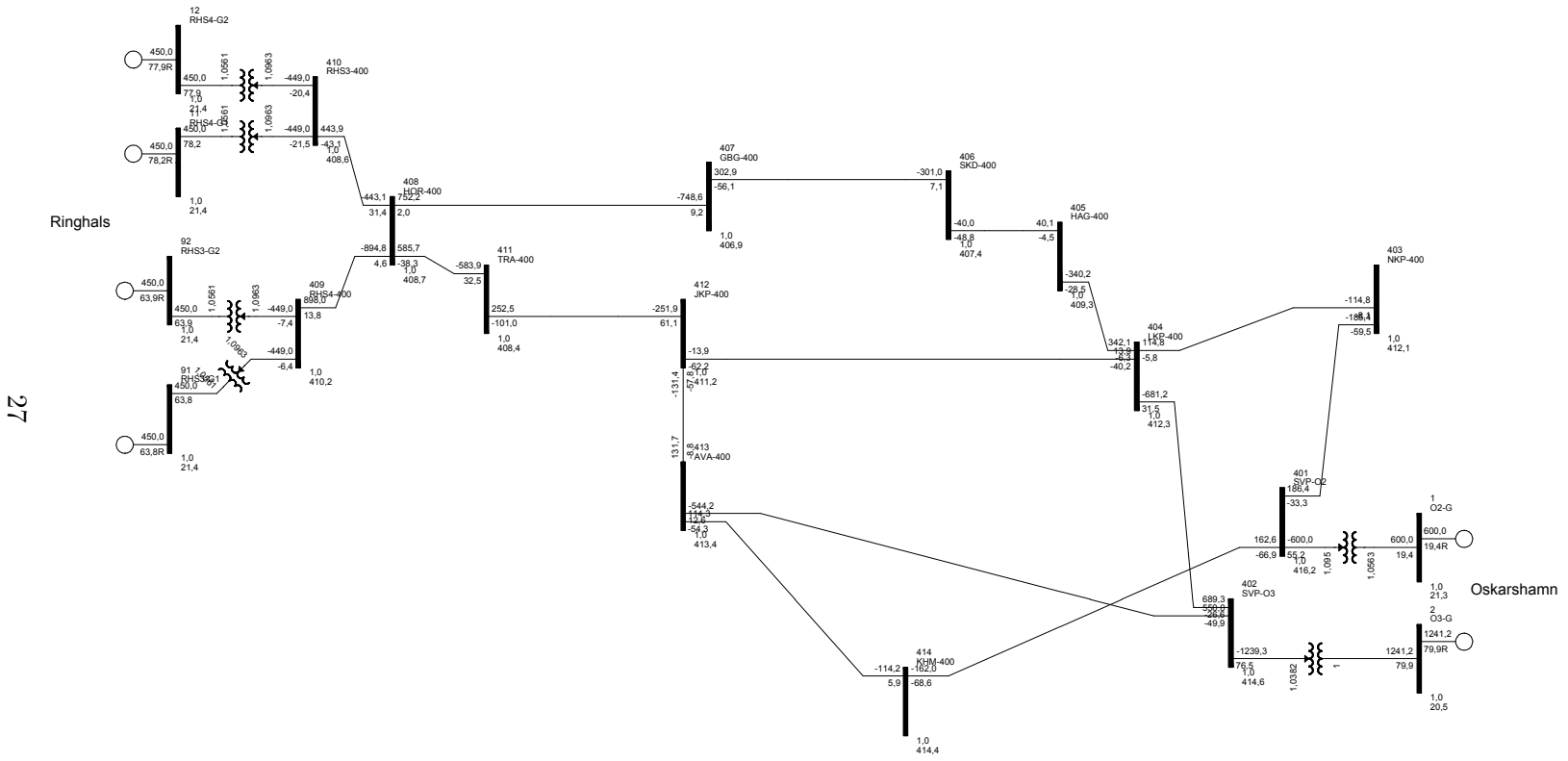


Figure 3.1: 400 kV power system

Out of the 14 400 kV substations only 10 of them connects to a 135 kV grid. The substations for the 135 kV grid are assumed to have the same geographical position and grounding as their 400 kV counterpart. There is also one transformation to 200 kV. The main objective of this 135 kV grid is to be able to connect loads to the system thus making the power system as authentic as possible. No transformations from 135/10 kV will be made. The interconnections in the 135 kV grid can be seen in Table.A.5 as well as the needed information for *GIC* analysis such as the DC resistive component.

The complete schematic of the 135 kV grid can be seen in Fig.3.2. The loads connected to the system which set the initial demand for the generators are presented in Table.A.6 including both the 135 kV and the 200 kV loads.

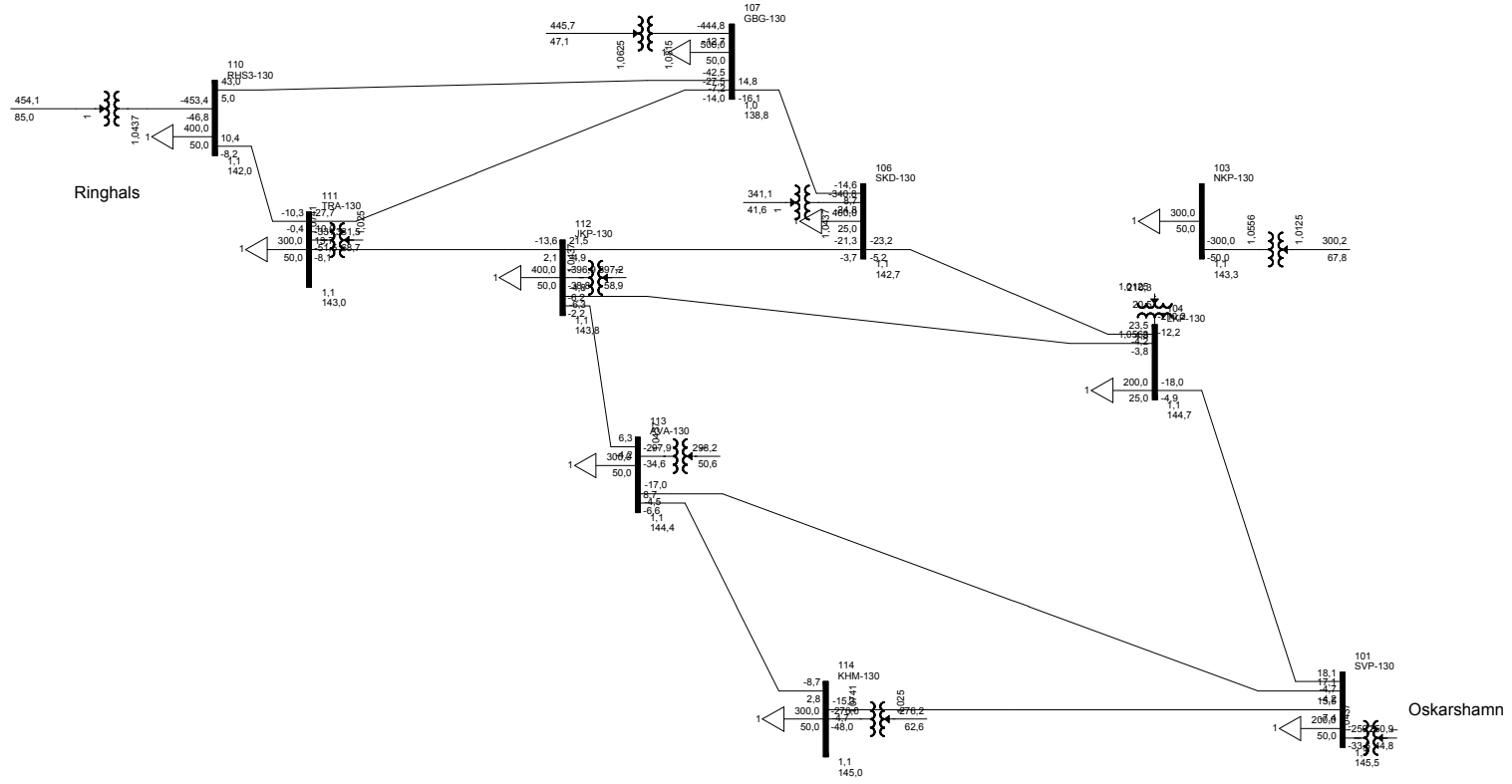


Figure 3.2: 135 kV system

3.2 GIC Simulations

The simulations performed were done to evaluate the *GIC* module and determine the effects *GIC* disturbances have on the power system used for evaluation. As the disturbances are in relation with reactive power losses these were the main target for evaluation. The tests considered the power system setup in the early 90's and the setup today as changes regarding transformer units have changed over time.

3.2.1 Simulation Prerequisites

For the simulations conducted, three different electric field magnitudes were used, 5, 10 and 20 V/km . The values were based on earlier tests where it had been noticed that a peak of 14 V/km had occurred in Sweden during the storm of 1989 [28]. The values were chosen to represent three storm scenarios with different severity.

In relation to the electric field magnitude the simulations are done for storm direction interval of $0-360^\circ$ stepped with 10° . As an indication of at which storm direction degree the worst *GIC* disturbances would appear. It was decided that a stepped interval of 10° would be sufficient for the analysis.

The simulations made are to determine reactive power losses and the currents created in the system to be able to analyze the impacts from *GIC* disturbances. The transformers were the main target of evaluation as they can be severely affected by these disturbances due to half cycle saturation.

3.2.2 Simulation Case

The simulations are performed for two cases, one representing the power system of the early 90's and the other how the power system is today. The difference between the two cases is transformer updates and an implementation of a *GIC* blocking resistance.

The transformer setup for the simulations regarding the power system in the early 90's are presented in Table.A.4. These simulations are performed to analyze the effects from the *GIC* disturbances in relation to the reactive power losses.

The setup for the power system today with updated transformer units for Gothenburg, Jönköping and implementation of a blocking resistance at Oskarshamn are presented in Table 3.1. The simulations are performed to find out if the changes made had improved the protection for *GIC* and how the reactive power losses had been affected.

The blocking resistance implemented at Oskarshamn (O3) is a resistance of 2.5Ω which increased the winding resistance from 0.079Ω to 7.579Ω . The change in winding resistance and how the blocking resistance is implemented are described in Section.2.7.1. As the resistance thereby had increased the impacts it would have on the disturbances

caused by *GIC* these needed to be investigated. Therefore tests were performed to evaluate the effects of the implementation of the blocking resistance. However the evaluation of the blocking resistance impact only regarded the *GIC*.

Table 3.1: The updated transformer units

Bus number	Name	W_1/W_2 [Ω]	Vector group	Core	$k - factor$
402	O3	7.579/-	YND1	Single phase	1.18
407	GBG	0.09/0.043	YNA0	3-phase 3-leg	0.29
412	JKP	0.1306/0.0369	YNA0	3-phase 3-leg	0.29

3.2.3 AC- vs DC-resistance

For accurate simulation results the DC-resistance values for the branches were acquired. However if these values would not been able to acquire it was decided to simulate the difference in effect of using the AC-resistance values. For the case with updated transformer units and implementation of blocking resistance a simulation is performed with AC- and DC-resistance values at an electric field magnitude of $10 V/km$ and storm direction at $0 - 360^\circ$. The data for the branches can be seen for the $400kV$ system in Table.A.2 and for the $135kV$ system in Table.A.5. The evaluation will only regard the total reactive power losses.

3.2.4 Power System Stability

As the outputs generated by the *GIC* module does not consider how well the power system withstands the *GIC* disturbances a *GIC Data Case Output File*, see Section.2.9.2, is created. The file is used in order to convert the reactive power losses into reactive current loads. The reactive current loads can then be loaded into the power system and be used for power flow simulations to determine the voltage levels at the substations.

4

Results

Simulations were run for several different cases. The section will start by presenting the results for the early 90's power system followed by results performed on the power system today. Comparison between the two will be presented and finally the impact on voltage stability will be presented.

4.1 Simulations

Starting with the power system from the early 90's the first simulation was made for the total reactive power demand. The simulation was performed with the electric field direction orienting from $0 - 360^\circ$ as well as varying the electric field magnitude in three steps, 5,10 and 20 V/km . The results can be seen in Fig.4.1. The simulations show an maximum increase in reactive power demand at 60° which for 10 V/km reaches 2191 $Mvar$.

In order to understand the impact of the different core designs of the transformers individual results need to be presented. The effective $GIC/phase$ for all transformers can be seen in Fig.4.2. Here the 400/135 kV transformer at Norrkoping (NKP) is subjected to the highest effective GIC peaking at 732 A . This is a result of NKP's low series winding resistance together with having the lowest substation ground resistance. Gothenburg (GBG) has the second highest current peaking at 476 A .

In Fig.4.3 the reactive power losses for each transformer is presented. Even though the current is highest for the transformer at NKP it can be seen that the transformers using single phase cores, O3 and GBG, have the highest losses with GBG peaking at 562 $Mvar$ for an electric field of 10 V/km . It can also be noted that the minimum value of the total losses in Fig.4.1 occurs when GBG has its minimum value.

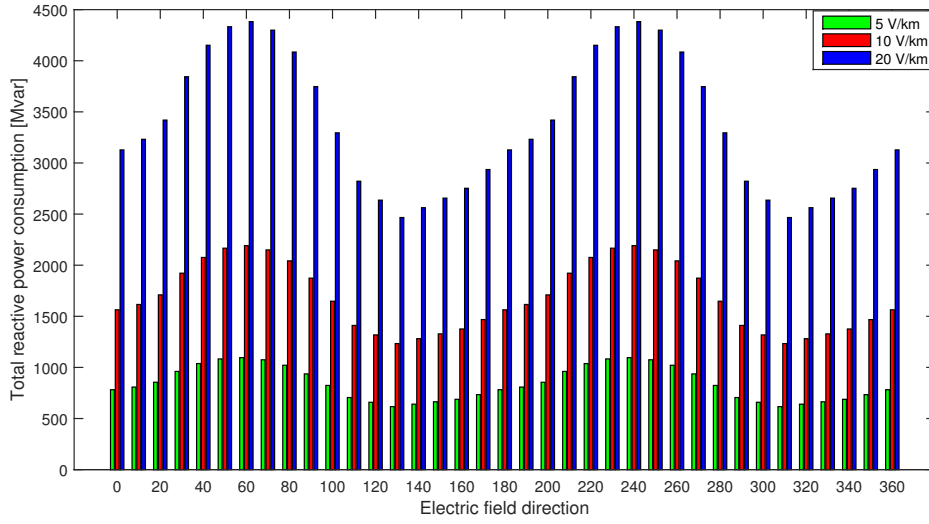


Figure 4.1: Total system losses]

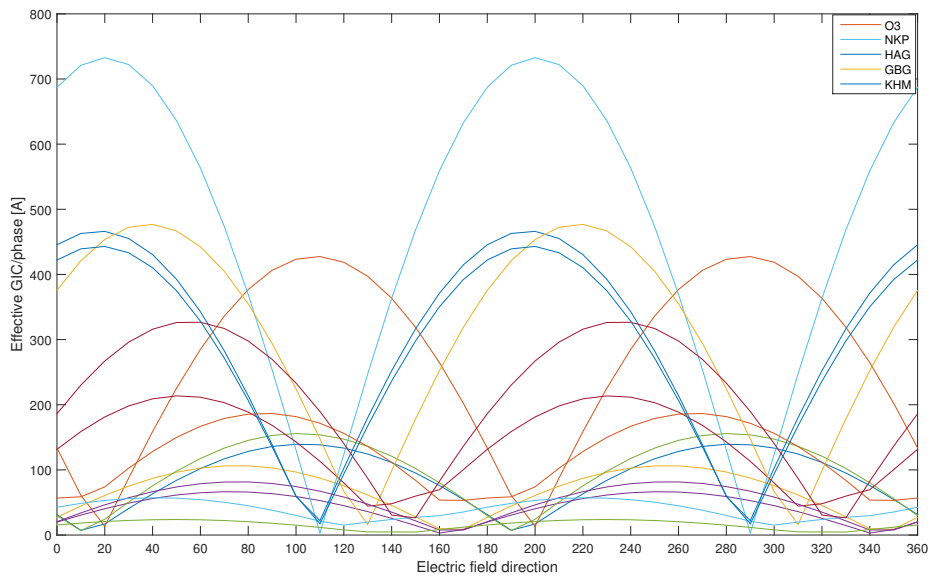


Figure 4.2: Individual effective GIC/phase for $E = 10 \text{ V/km}$

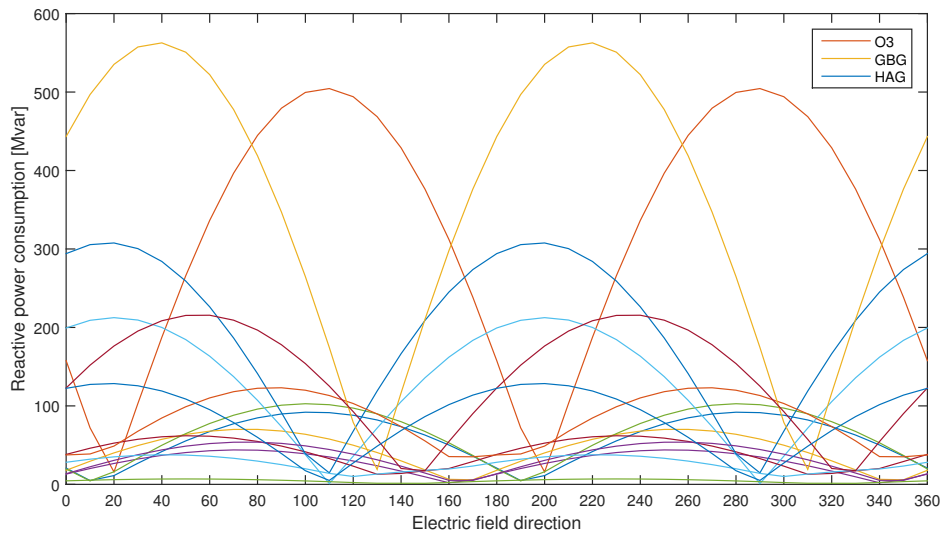


Figure 4.3: Individual transformer losses for $E = 10 \text{ V/km}$

For the worst case where the reactive power losses are the largest the 400kV system is depicted in Fig.4.4. The storm direction at 60° is visualized with arrows and each substation current flow to ground is shown. These currents are the results of a storm with electric field magnitude of 10V/km . The simulation giving the result is a basic nodal analysis to find out the the current flow between substation and substation ground to see what current magnitude the substation will be exposed to at the given case. The sum of all the currents results in zero.

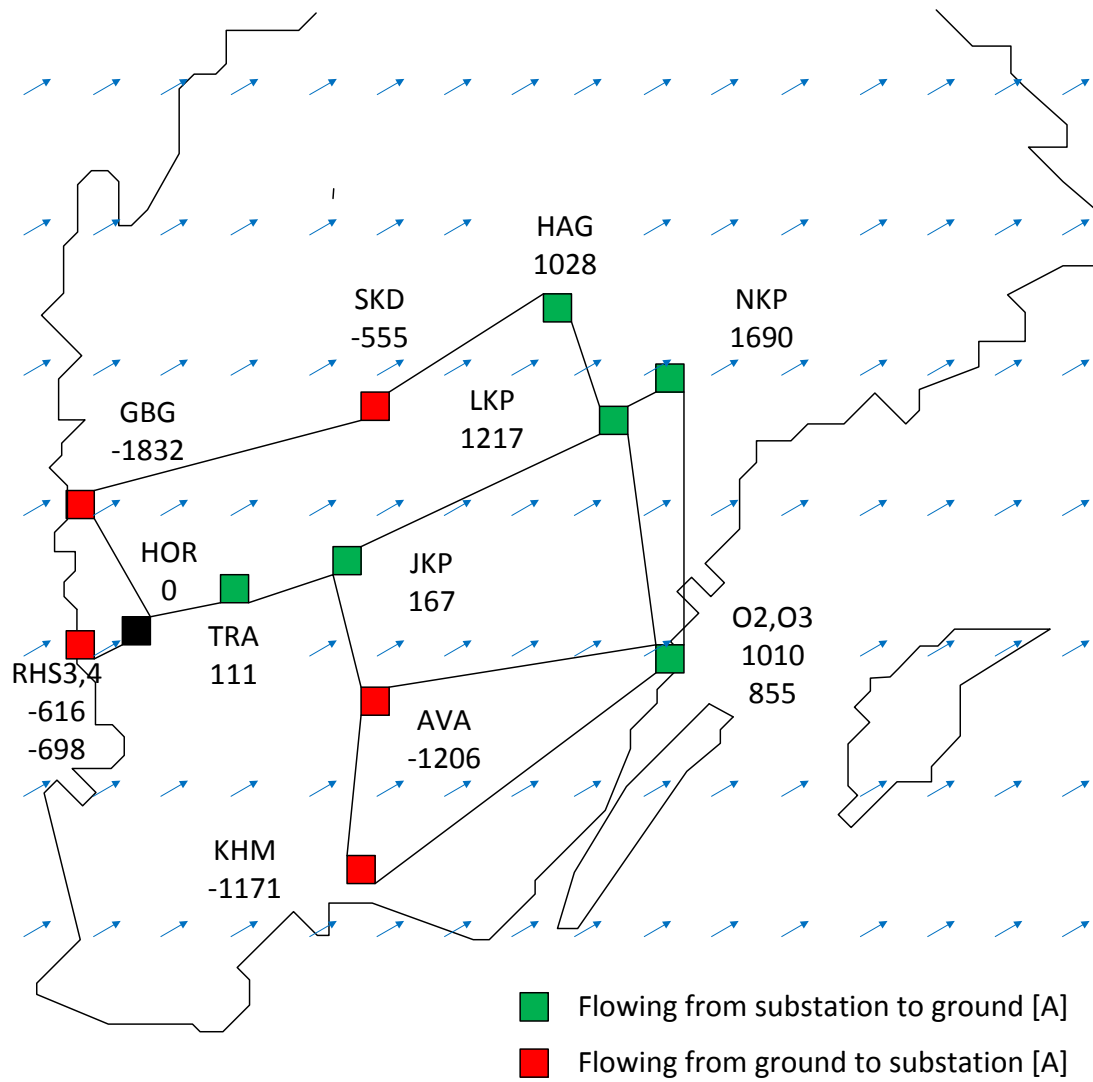


Figure 4.4: Sweden storm direction 60° current flow from substation to ground

4.2 Updated power system

This section will present the results from the simulations performed for the power system as it is today. The changes made are the transformers connected to O3, GBG and JKP. O3 has received a *GIC* blocking resistance of 2.5Ω connected to the HV neutral path. How this is implemented and the effects are described in Section.2.7.1. GBG and JKP have both had their transformers replaced with 3-phase 3-leg core type transformers. The total reactive power consumption can be seen in Fig.4.5. For the new system the maximum reactive power consumption is reached at 50° which results in 1498 Mvar for 10 V/km . For the first case this peak occurred at 60° storm direction where the reactive power losses were dominated by GBG and O3. With the implemented changes to the transformers the losses are more evenly distributed and as a result the peak now occurs at 50° storm direction.

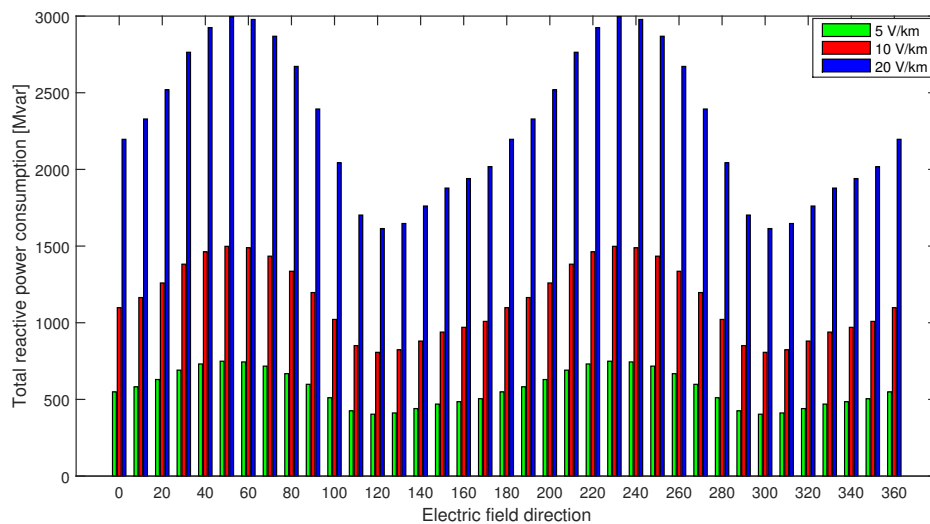


Figure 4.5: Total system losses

The implementation of a blocking resistor at Oskarshamn 3(O3) will affect the currents through all transformers. The effective *GIC/phase* for the transformers can be seen in Fig.4.6. NKP still has the highest current peaking at 736 A . Even though no changes were made to the transformer at NKP the current has still increased. This is due to the blocking resistor at O3 deflecting the current to other substations. The current in GBG has also increased after the installment of a 3-phase 3-leg core typ transformer and will be discussed more in Subsec.4.2.1.2. The blocking resistor at O3 has had the desired effect and its current has decreased significantly and is given in more detail in Subsec.4.2.1.1.

The individual power losses are shown in Fig.4.7. O3 and GBG are no longer dominant for the power losses. Instead HAG, NKP and AVA have the highest losses with the 400/200 kV transformer at HAG having the highest peak of 309 Mvar for an electric

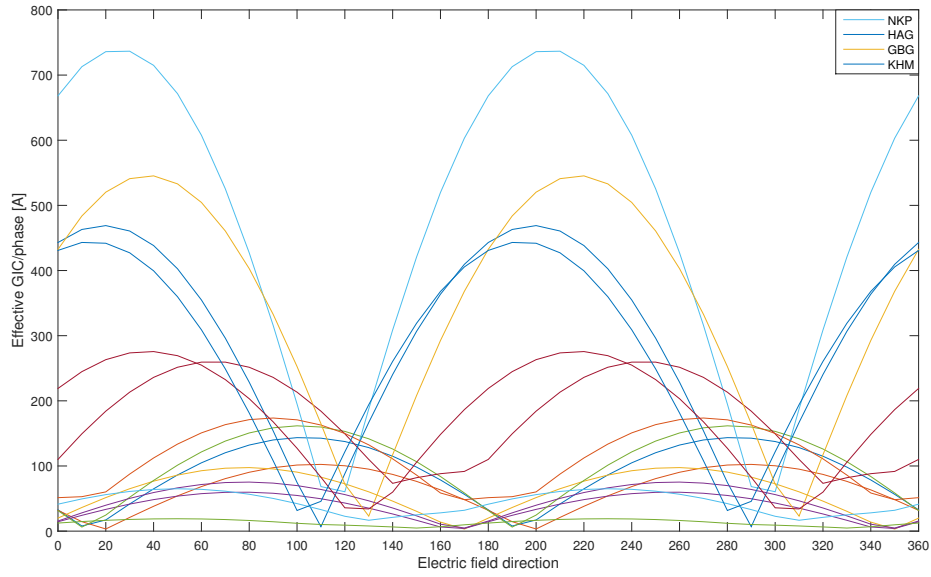


Figure 4.6: Individual effective GIC/phase for $E = 10 \text{ V/km}$

field of 10 V/km . Even though the effective $GIC/phase$ is higher for NKP the 3-phase 5-leg core type transformer at HAG is less capable of dealing with the GIC resulting at higher reactive power losses.

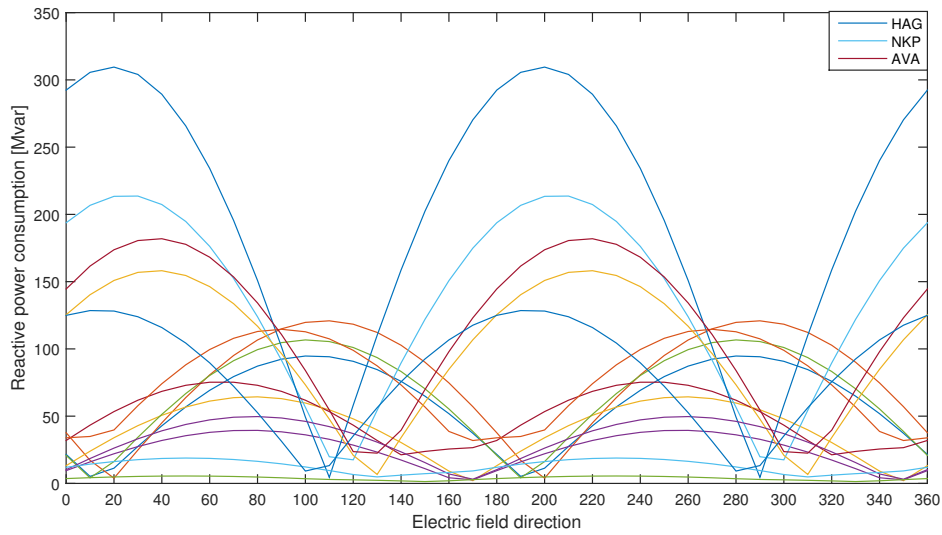


Figure 4.7: Individual transformer losses for $E = 10 \text{ V/km}$

As for the case where the old transformer units were used, the simulations for the new current flow from substation to ground can be seen in Fig.4.8 for an electric field magnitude at $10V/km$ with a storm direction of 50° . The most noticeable is that if comparing the the worst cases Fig.4.4 with Fig.4.8 is the current flowing from substation to ground at Oskarshamn (O3) has decreased from 855 A to 162 A.

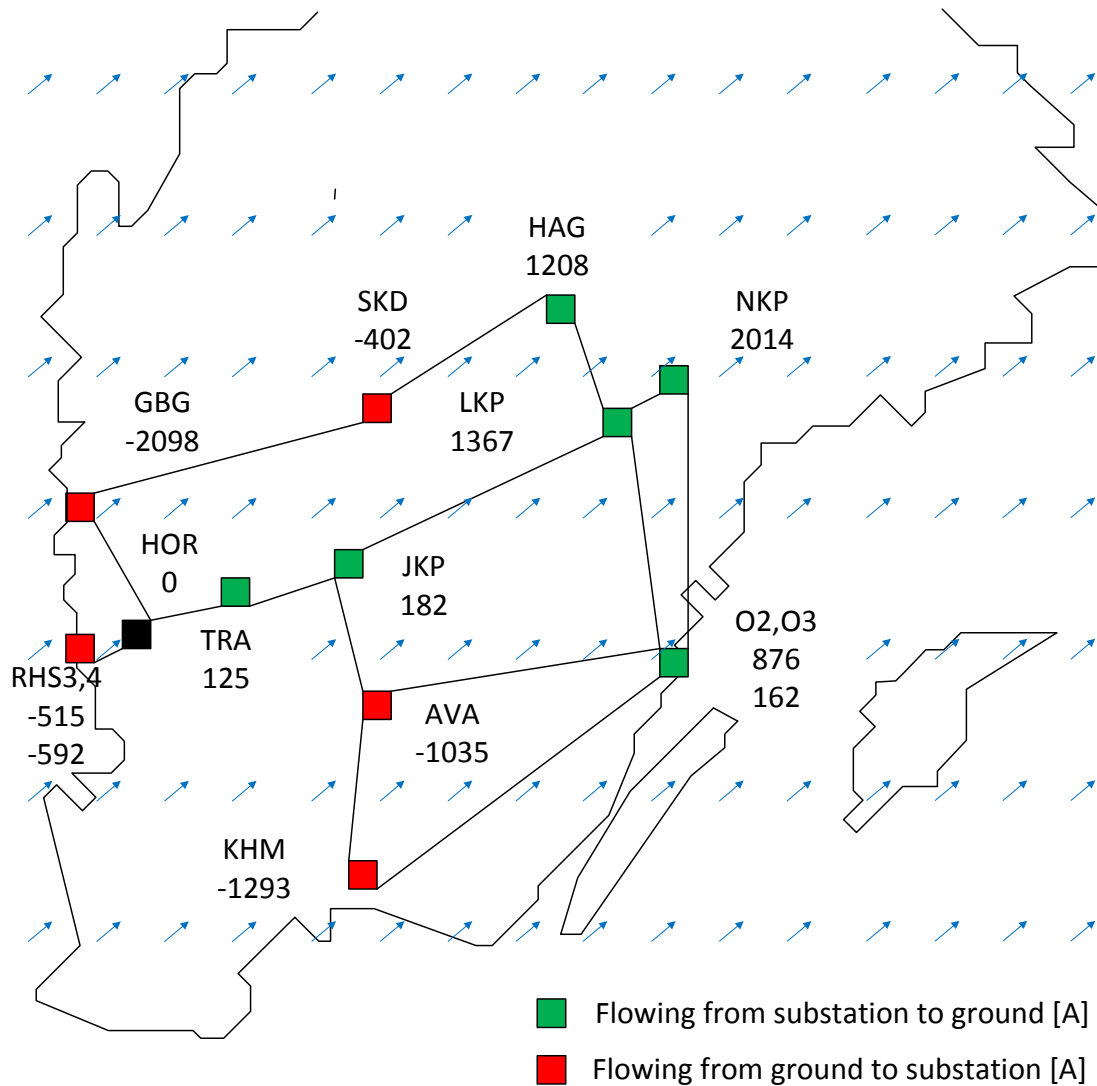


Figure 4.8: Sweden storm direction 50° current flow from substation to ground

4.2.1 Comparison of the changes between the two power system

This section will compare the changes made to the power system. Specifically O3,JKP and GBG will be presented. All simulations have been done with a constant electric field of 10 V/km .

4.2.1.1 Oskarshamn 3

For the early 90's power system O3 had the second highest reactive power demand in the power system. With a effective GIC at 427 A and a reactive power loss at 504 Mvar, the simulations for O3 gave similar results to historical values. The effective GIC and the reactive power losses for O3 have been found to be 403 A and 391 Mvar respectively [29]. The difference for the current is approximately 6% while the difference for reactive power loss is about 30%.

When implementing a blocking resistance on the neutral of the HV winding for O3 the reactive power consumption was greatly reduced. This can be seen in Fig.4.9. The reactive power demand dropped from 504 Mvar to 102 Mvar.

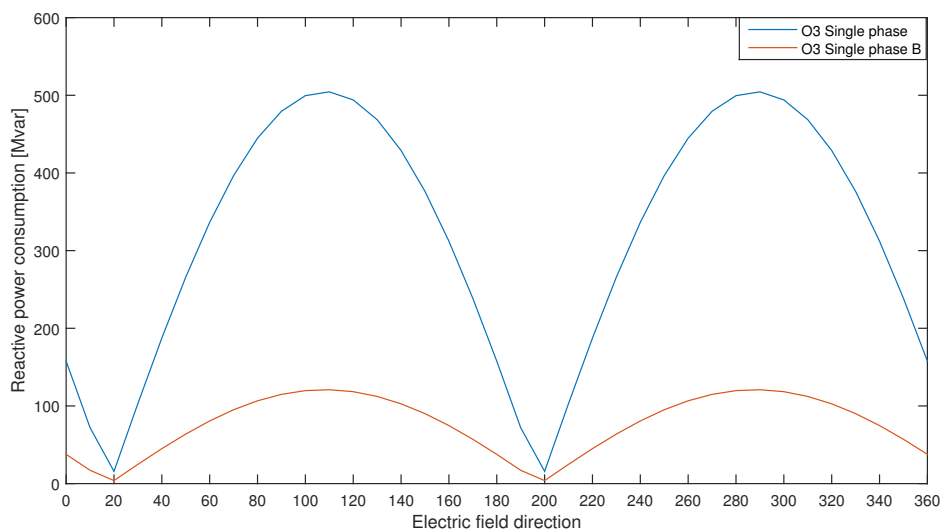


Figure 4.9: Reactive power losses for Oskarshamn 3 with and without blocking resistor

In Fig.4.10 the current in the transformer, effective GIC /phase, is shown. The blocking resistance reduces the current by 325 A. However even though the blocking resistance has decreased the current flowing in the neutral of O3 it will redirect the flow of GIC to other parts of the power system.

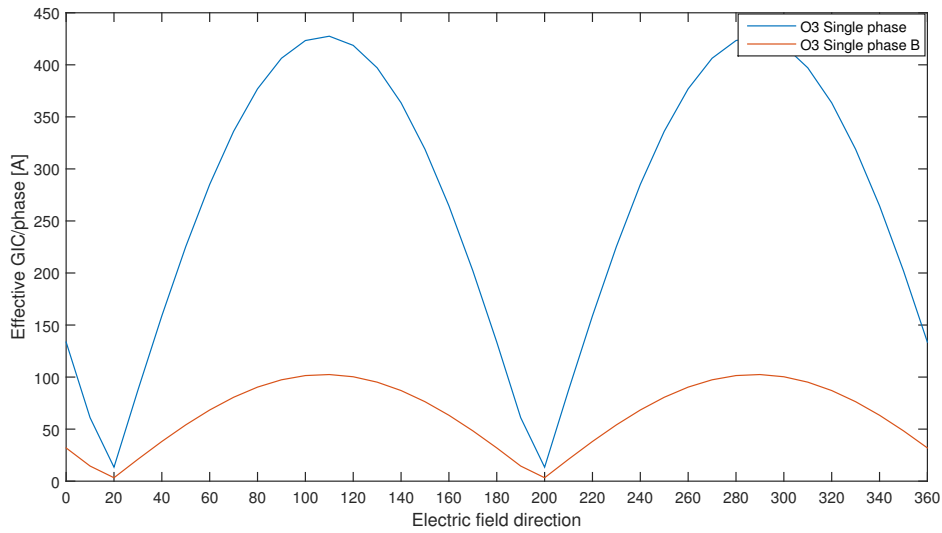


Figure 4.10: Transformer GIC effective/phase

4.2.1.2 Gothenburg

GBG had the highest Mvar consumption in case one. When changing the transformer core type from a single phase to a 3-phase 3-leg the reactive power consumption decreased. This is presented in Fig.4.11. The reactive power consumption has decreased from 562 Mvar to 158 Mvar.

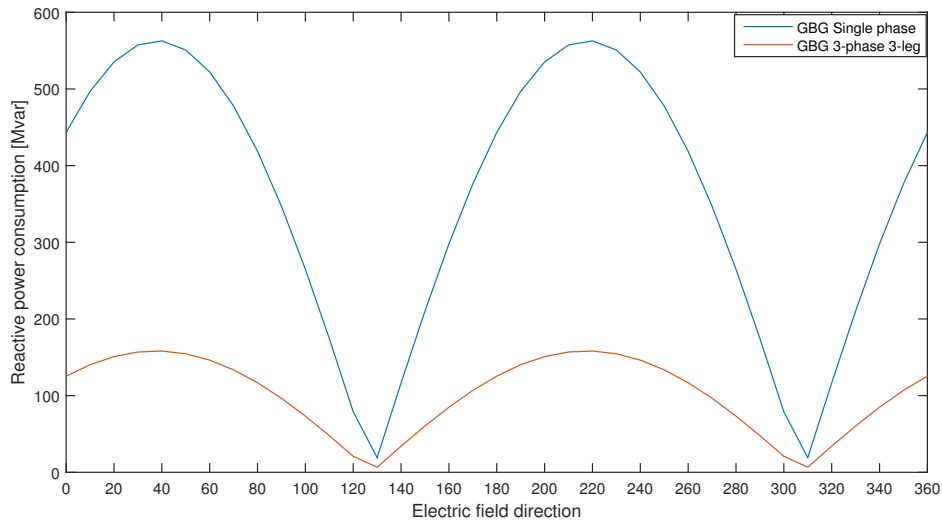


Figure 4.11: Transformer losses for Gothenburg [Mvar]

The effective $GIC/phase$ is shown in Fig.4.12. Even though reactive power consumption has decreased the effective $GIC/phase$ has increased when substituting the transformer to a 3-phase 3-leg core type. This is due to the series winding resistance being lower for the 3-phase 3-leg core type.

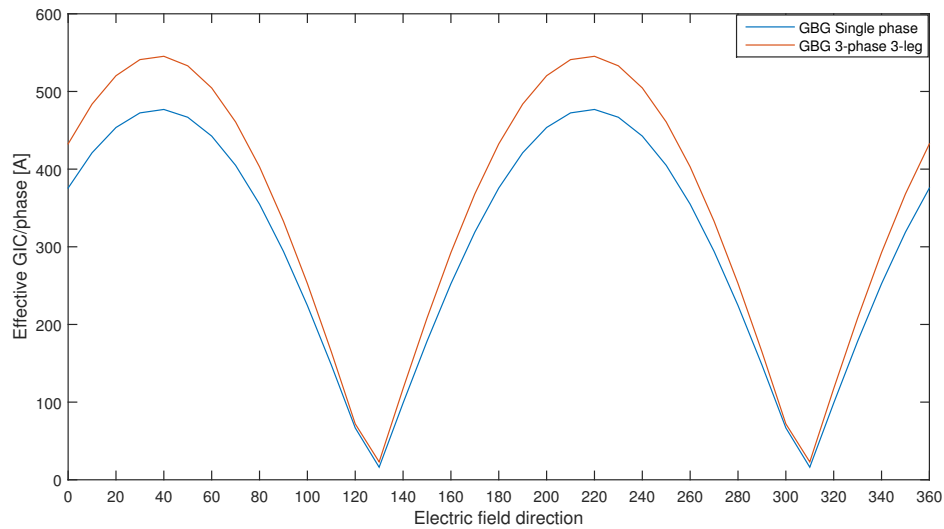


Figure 4.12: Transformer GIC effective/phase

4.2.1.3 Jönköping

For JKP, the transformer core type was changed from a 3-phase 5-leg to a 3-phase 3-leg core type transformer. The reactive power demand can be seen in Fig.4.13. Even though the 5-leg core type is adequate with dealing with GIC the reactive power demand drops from 37 $Mvar$ to 5 $Mvar$. However here a phase shift can be noticed on the peaks.

When examining the effective $GIC/phase$ in Fig.4.14 the same phase shift is evident. The reason for this phase shift is the blocking resistance installed at O3 for the new power system. When using a blocking device it will redistribute the GIC flow in the system. As seen in Fig.4.10 O3 has its maximum values at 120° which is the old minimum point for JKP. Here the blocking resistance will impact the system the most. The current redirected to JKP is large enough to shift the minimum point by 10° .

4.2.2 Comparison between AC and DC branch data

To find out how huge impact the difference in AC- and DC-resistance values for the branches simulations were performed with electric field magnitude at $10V/km$ and storm direction $0 - 360^\circ$ to find out the difference in reactive power losses. The results are given in Fig.4.15 At 100° and 280° a difference for the reactive power losses peaked with 12.79%. At these storm directions the lines connecting Horred (HOR) and Ringhals drew

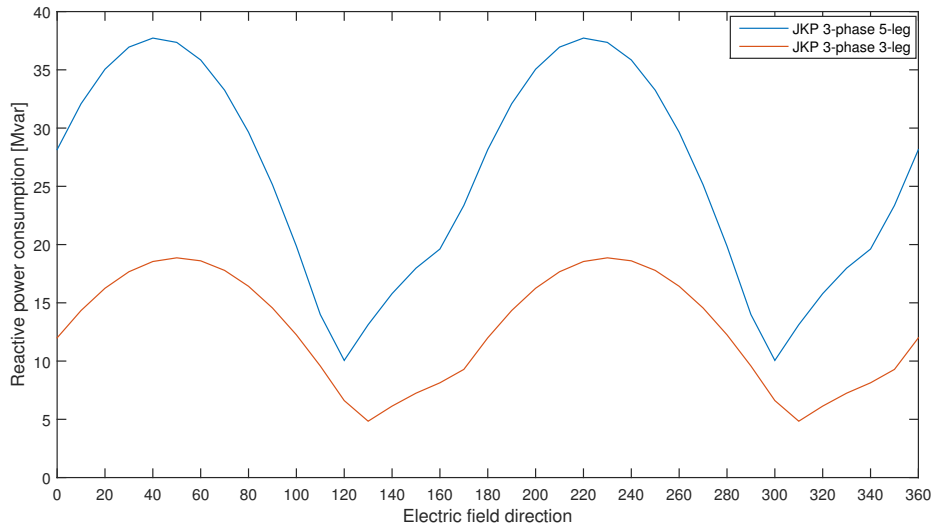


Figure 4.13: Reactive power losses for Jonkoping [Mvar]

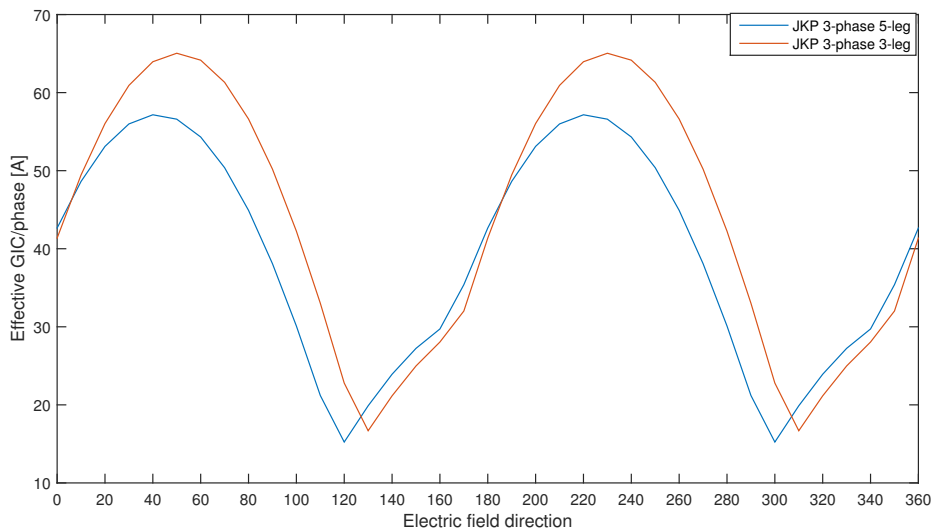


Figure 4.14: Transformer GIC effective/phase

its largest currents. These lines also had the highest difference between their resistive AC and DC-values and as a result also the highest difference in reactive power consumption. The smallest difference were at 10° and 190° where the reactive power losses only differ 0.97%. The average difference in reactive power loss between using AC- and DC-resistance values for the branches were 6.8%.

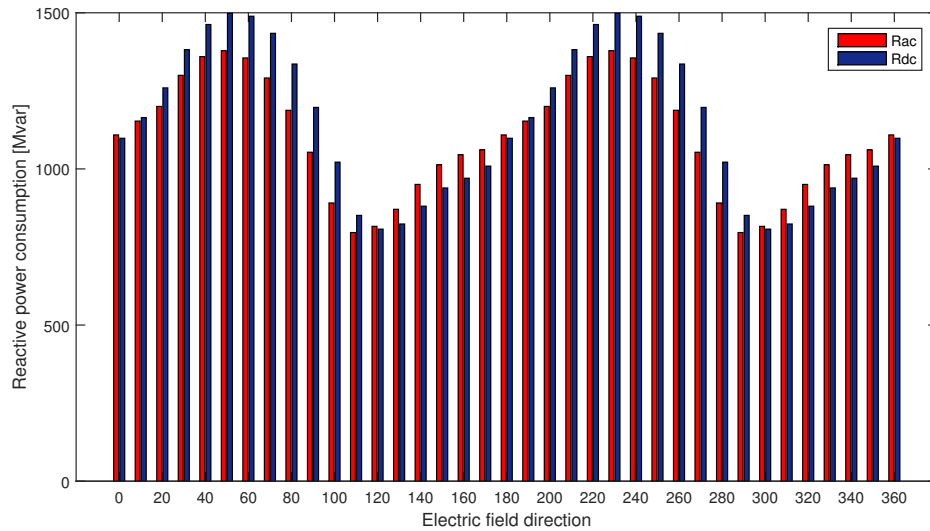


Figure 4.15: Total reactive power losses in the system for AC- vs DC-resistive components of the branches

4.2.3 Power system analysis

In order to understand how the increased losses in the transformers impact the power system a power flow analysis was made. The *GIC* event chosen was for maximum losses at an electric field of 10 V/km . Since the current load MVA can be high compared to ordinary load flow constant P-, Q-load it is recommended that the *PSS/E* switching activities are used in the following order:

1. CONG
2. CONL
3. Read GIC RDCH file
4. ORDR
5. FACT
6. TYSL

The resulting voltage drops for the 400 kV can be seen in Fig.4.16. Here the voltage in blue is the voltage (p.u) during normal operation while the red voltage represent the voltage (p.u) during the *GIC* event.

44

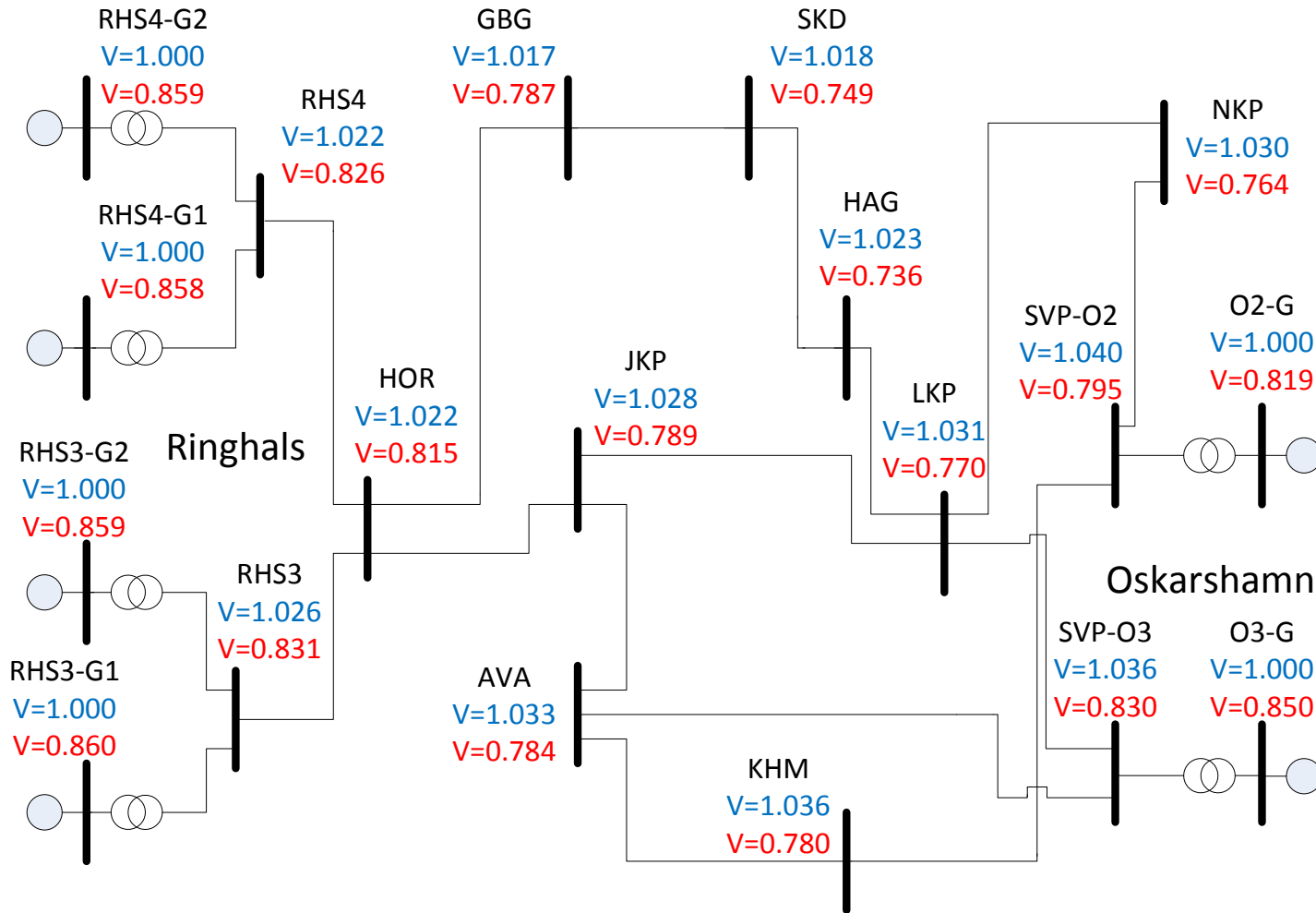


Figure 4.16: Influence on the voltage stability of the 400 kV system during a GIC event

5

Discussion

The simulations were performed using the student version of PSS/E. The student version is limited to a 50 bus system. Therefore when designing the power system the bus limit had to be taken into account. Since Oskarshamn 3 has had previously documented issues regarding *GIC* disturbances it was chosen as the main part of this investigation. This meant that compromises had to be made for other areas. Gothenburg for instance is represented in the power system as a single substation, when in fact there are several for the Gothenburg area. Therefore the substations is subdued to the full impact of the *GIC* while in reality it would be divided amongst several others.

From the results it was concluded that the simulated reactive power losses for O3 did not concur with the acquired data. The predetermined values for the *k-factor* was used for the simulations and it should be taken into account that they are based on older transformer models and simplifications for reactive power loss calculations. Here the *k-factor* represents the linear relationship between the fundamental component of the current and the reactive power losses. However, the *GIC* module offers the user to change the *k-factor*. This offers the user more flexibility as better values from updated transformer models can be inserted. This makes it possible to include the size of the transformer and not only its nameplate information.

When it comes to the application window for the *GIC* module a few implementations would enhance the user experience. In order to get as accurate results as possible the DC-components needs to be used. At the moment, the data for transmission lines are not entered in the *GIC* file, instead the data from the sav file is used. This means that the user has to manually change the data if the DC-components are available. It would be more appropriate to have the AC-components in the sav file and give the user the option to put in the DC-components for the transmission lines in the *GIC* file. Thereby the DC-components would be used for the *GIC* simulation and the AC values would be

used for other simulations in PSS/E.

When regarding the blocking devices the *GIC* file offers limited options. The user have the option to either active or deactivate a blocking device on a transformer neutral winding. When activated it completely blocks the *GIC* in the neutral. A more appropriate solution is to allow the user to input a resistive value and therefore determine if it should completely block or just reduce. Taken the simulated cases for O3 into account were a blocking resistance was added, this had to be done manually by adding its resistive value into the series resistance value of the transformer.

The impact that the reactive losses would have on the voltage stability was also analyzed. The voltage drops obtained from the simulations should however be taken with moderation. In order to get realistic results the robustness of a larger power system needs to be used. Any form of compensation was also not included during the simulations.

It should also be noted that the power system used is run at 50 Hz. At 50 Hz the difference between the resistive AC value and DC value for branches is smaller than for 60 Hz. Therefore another analysis needs to be made with 60 Hz in order to be able to conclude if the AC values are accurate enough for simulations.

6

Conclusion

The *GIC* module in *PSS/E* has been evaluated for a power system illustrating the mid to south parts of Sweden. The power system was designed in order to give an as accurate representation of Oskarshamn 3 (O3) as possible in order to recreate previously noted problems.

The simulations performed with the *GIC* module made it possible to examine the impact of the storm direction. Simulations showed that the total reactive power losses could differ up to 46% depending on the storm direction. The *GIC* module also made it possible to visualise the impact of the individual transformers in order to detect which transformers impact the system the most. It could be concluded that even though the effective *GIC* in the single phase transformers were lower than for other core types they still had the highest reactive power losses. From the individual results it could also be concluded that the 3-phase 3-leg core type transformer was the least susceptible to *GIC*. After implementing changes to the two single phase transformers as well as a 3-phase 5-leg transformer the maximum total reactive power loss in the system was reduced by 31%.

The module was also used in order to analyze the difference between AC and DC resistive values of the branches. The simulations showed an average difference of 6.8% in the total reactive power losses. It can therefore be concluded that the resistive AC values of the branches can be used with adequate results in order to estimate the reactive power losses.

The simulations performed for Oskarshamn 3 (O3) showed a difference in the effective *GIC* of 6% compared to previously acquired data. The simulated reactive power loss for O3 was 30% higher than previously acquired data. It can therefore be concluded that the *GIC* module is sufficient to represent the stress in form of effective *GIC* that the transformers are subjected to. However the default values used in order to calculate the

reactive power losses are not accurate enough. If the *GIC* module is used in order to analyze the reactive power losses the individual *k* – *factors* need to be reevaluated.

References

- [1] I. CENTRA Technology, Geomagnetic storms (2011) 9–13, 18, 22.
- [2] S. Lindahl, Effect of geomagnetically induced currents on protection systems (2003) 7–8, 10–12.
- [3] Courtesy of soho/lasco c2, soho/eit 304 consortium. soho is a project of international cooperation between esa and nasa.
- [4] Courtesy of soho/mdi consortium. soho is a project of international cooperation between esa and nasa.
- [5] L. Bolduc, P. Langlois, D. Boteler, R. Pirjola, A study of geoelectromagnetic disturbances in quebec. ii. detailed analysis of a large event, Power Delivery, IEEE Transactions on 15 (1) (2000) 277.
- [6] S. Lindahl, Effect of geomagnetically induced currents on protection systems (2003) 2, 13.
- [7] J. Kappenman, A perfect storm of planetary proportions, Spectrum, IEEE 49 (2) (2012) 29–31.
- [8] I. CENTRA Technology, Geomagnetic storms (2011) 19.
- [9] Application guide computing geomagnetically-induced current in the bulk-power system 5–7,28.
- [10] S. Lindahl, Effect of geomagnetically induced currents on protection systems (2003) 49.
- [11] F. Sui, A. Rezaei-Zare, M. Kostic, P. Sharma, A method to assess gic impact on zero sequence overcurrent protection of transmission lines, in: Power and Energy Society General Meeting (PES), 2013 IEEE, 2013, pp. 1–2.

- [12] A. P. S. D. Metatech, Evaluation of the vulnerability of the satnett and svenska kraftnat transmission networks to the effects of geomagnetic storms part 1 - studies and analyses (2000) 6–3.
- [13] A. P. S. D. Metatech, Evaluation of the vulnerability of the satnett and svenska kraftnat transmission networks to the effects of geomagnetic storms part 1 - studies and analyses (2000) 6–1.
- [14] S. Lindahl, Effect of geomagnetically induced currents on protection systems (2003) 167.
- [15] A. P. S. D. Metatech, Evaluation of the vulnerability of the satnett and svenska kraftnat transmission networks to the effects of geomagnetic storms part 1 - studies and analyses (2000) 6–4.
- [16] A. P. S. D. Metatech, Evaluation of the vulnerability of the satnett and svenska kraftnat transmission networks to the effects of geomagnetic storms part 1 - studies and analyses (2000) 6–5.
- [17] A. Rezaei-Zare, Enhanced transformer model for low- and mid-frequency transients 2014;part ii: Validation and simulation results, Power Delivery, IEEE Transactions on PP (99) (2014) 2.
- [18] S. A. Mousavi, Electromagnetic modelling of power transformers with dc magnetization, qC 20121121 (2012).
- [19] T. S. Molinski, Why utilities respect geomagnetically induced currents, Journal of Atmospheric and Solar-Terrestrial Physics 64 (16) (2002) 1770, space Weather Effects on Technological Systems.
URL <http://www.sciencedirect.com/science/article/pii/S1364682602001268>
- [20] R. Girgis, K. Vedante, Effects of gic on power transformers and power systems, in: Transmission and Distribution Conference and Exposition (T D), 2012 IEEE PES, 2012, pp. 1–8.
- [21] Application guide computing geomagnetically-induced current in the bulk-power system 24–25.
- [22] C. Mao, S. Wang, J. Lu, G. Mei, D. Wang, Measures of restraining dc current through transformer neutral point: A comprehensive survey, in: Universities Power Engineering Conference, 2007. UPEC 2007. 42nd International, 2007, p. 709.
- [23] Application guide computing geomagnetically-induced current in the bulk-power system 22–23.
- [24] Application guide computing geomagnetically-induced current in the bulk-power system 27–28.

- [25] Application guide computing geomagnetically-induced current in the bulk-power system 26–26.
- [26] X. Dong, Y. Liu, J. Kappenman, Comparative analysis of exciting current harmonics and reactive power consumption from gic saturated transformers, in: Power Engineering Society Winter Meeting, 2001. IEEE, Vol. 1, 2001, pp. 318–322 vol.1.
- [27] Siemens, Pss/e 33.4 program operation manual (2013) 7–1 – 7–6.
- [28] A. P. S. D. Metatech, Evaluation of the vulnerability of the satnett and svenska kraftnat transmission networks to the effects of geomagnetic storms part 1 - studies and analyses (2000) 7–10, 8–10.
- [29] A. P. S. D. Metatech, Evaluation of the vulnerability of the satnett and svenska kraftnat transmission networks to the effects of geomagnetic storms part 1 - appendices (2000) G19.

A

Appendix

A.1 400 KV Power System input data

Table A.1: 400 kV Substation coordinates

Bus number	Name	GPS Coordinates	Latitude N	Longitude E	Ground [Ω]
401	O2	57°24'30"N 16°38'59"E	57.4083°	16.6497°	0.25
402	O3	57°24'50"N 16°39'50"E	57.4139°	16.6639°	0.25
403	NKP	58°42'40"N 15°56'40"E	58.7111°	15.9444°	0.04
404	LKP	58°24'50"N 16°39'50"E	58.5367°	15.9500°	0.28
405	HAG	59°2'2"N 14°56'3"E	59.0339°	14.9342°	0.27
406	SKD	58°32'N 13°43'E	58.0089°	13.0001°	0.22
407	GBG	57°48'N 12°20'E	57.0001°	12.0001°	0.105
408	HOR	57°22'40"N 12°33'30"E	57.3778°	12.5583°	0.35
409	RH3	57°15'32"N 12°6'34"E	57.2589°	12.1094°	0.18
410	RH4	57°15'26"N 12°6'41"E	57.2572°	12.1114°	0.18
411	TRA	57°28'11"N 13°10'12"E	57.4697°	13.1700°	0.8
412	JKP	57°40'54"N 14°11'26"E	57.6817°	14.1906°	0.66
413	AVA	56°51'47"N 14°29'58"E	56.8631°	14.4994°	0.15
414	KHM	56°19'18"N 14°42'45"E	56.3217°	14.7125°	0.3

Table A.2: 400 kV branch data

Bus number	Cable type	Cable length[km]	R_{ac} p.u	X_{ac} p.u	B_{ac} p.u	R_{dc} p.u
401-403	2*593 Curlew	170	0.030813	0.350625	0.097143	0.028688
401-414	3*593 Almg	200	0.02625	0.3375	0.133333	0.0225
402-413	3*593 Almg	156	0.020475	0.26325	0.104	0.01755
402-404	3*593 Almg	140	0.018375	0.23625	0.0933333	0.01575
403-404	2*593 Curlew	24	0.00435	0.0495	0.0137143	0.00405
404-405	2*593 Curlew	93	0.0168563	0.1918125	0.0531429	0.0156938
404-412	3*593 Almg	145	0.0190313	0.2446875	0.0966667	0.0163125
405-406	2*593 Curlew	90	0.0163125	0.185625	0.0514286	0.0151875
406-407	2*593 Curlew	120	0.02175	0.2475	0.0685714	0.02025
407-408	3*593 Almg	50	0.0065625	0.084375	0.0333333	0.005625
408-409	3*593 Almg	31	0.0040688	0.0523125	0.0206667	0.002258
408-410	3*593 Almg	31	0.0040688	0.0523125	0.0206667	0.002258
408-411	3*593 Almg	42	0.0055125	0.070875	0.028	0.004725
411-412	3*593 Almg	68	0.008925	0.11475	0.0453333	0.00765
412-413	3*593 Almg	98	0.0128625	0.165375	0.0653333	0.0336875
413-414	3*593 Almg	70	0.0091875	0.118125	0.0466667	0.007875

With $U_{base} = 400$ kV and $S_{base} = 1000$ MVA.

Table A.3: Generator data

Bus number	Name	S_{Base} [Mvar]	Q_{Max} [Mvar]
1	O2-G	700	200
2	O3-G	1256	∞
11	RH4-G1	550	150
12	RH4-G2	550	150
91	RH3-G1	550	150
92	RH3-G2	550	150

Table A.4: 400/135 kV Transformer data

Bus number	Name	W_1/W_2 [Ω]	Vector group	Core	$k - factor$
401	O2	0.2/-	YND1	Three phase 5-leg	0.66
401	O2	0.231/0.030	YNA0	Three phase 5-leg	0.66
402	O3	0.079/-	YND1	Single phase	1.18
403	NKP	0.1305/0.0364	YNA0	Three phase 3-leg	0.29
404	LKP	0.108/0.030	YNA0	Three phase 3-leg	0.29
405	HAG	0.0766/0.147	YNA0	Three phase 5-leg	0.66
406	SKD	0.127/0.01916	YNA0	Three phase 5-leg	0.66
407	GBG	0.325/0.055	YNA0	Single phase	1.18
409	RH3	0.293/-	YND1	Three phase 5-leg	0.66
409	RH3	0.2935/-	YND1	Three phase 5-leg	0.66
410	RH4	0.284/-	YND1	Three phase 5-leg	0.66
410	RH4	0.284/-	YND1	Three phase 5-leg	0.66
410	RH4	0.231/0.030	YNA0	Three phase 5-leg	0.66
411	TRA	0.207/0.058	YNA0	Three phase 3-leg	0.29
412	JKP	0.155/0.0241	YNA0	Three phase 5-leg	0.66
413	AVA	0.231/0.030	YNA0	Three phase 5-leg	0.66
414	KHM	0.132/0.040	YNA0	Three phase 3-leg	0.66

A.2 135 KV Power System input data

Table A.5: 135 kV branch data

Bus number	Cable type	Cable length[km]	R_{ac} p.u	X_{ac} p.u	B_{ac} p.u	R_{dc} p.u
101-104	1*910 Almg	160	0.3423868	3.2482853	0.0091125	0.3072702
101-113	1*593 Almg	150	0.4691358	3.1687243	0.0082841	0.4526749
101-114	1*593 Almg	203	0.6348971	4.2883402	0.0112111	0.6126200
104-106	1*593 Almg	180	0.562963	3.8024691	0.0099409	0.5432099
104-112	1*593 Almg	160	0.5004115	3.3799726	0.0088364	0.4828532
106-107	1*593 Almg	140	0.4378601	2.9574760	0.0077318	0.4224966
106-112	1*593 Almg	160	0.5004115	3.3799726	0.0088364	0.4828532
107-110	1*593 Almg	95	0.2971193	2.0068587	0.0052466	0.2866941
107-111	1*593 Almg	95	0.2971193	2.0068587	0.0052466	0.2866941
110-111	1*593 Almg	145	0.4534979	3.0631001	0.0080080	0.4375857
111-112	1*593 Almg	104	0.3252675	2.1969827	0.0057436	0.3138546
112-113	1*100Cu	122	1.2049383	3.0123457	0.0057014	1.1781619
113-114	1*593 Almg	63	0.1970370	1.3308642	0.0034793	0.1901235

With $U_{base} = 135$ kV and $S_{base} = 1000$ MVA.

Table A.6: The loads connected to the 135 kV busses

Bus number	Name	P_{load} [MW]	Q_{load} [Mvar]
101	SVP-130	200	50
103	NKP-130	300	50
104	LKP-130	200	25
106	SKD-130	400	25
107	GBG-130	500	50
110	RHS-130	400	50
111	TRA-130	300	50
112	JKP-130	400	50
113	AVA-130	300	50
114	KHM-130	300	50
205	HAG-200	300	25

A.3 GIC Data Input File

401,'O2-G ',1, 57.4080009, 16.6499996, 0.2500
402,'O3-G ',1, 57.4140015, 16.6639996, 0.2500
403,'NKP ',1, 58.7111092, 15.9443998, 0.0400
404,'LKP ',1, 58.5367088, 15.9499998, 0.2800
405,'HAG ',1, 59.0339012, 14.9342003, 0.2700
406,'SKD ',1, 58.0089035, 13.0001001, 0.2200
407,'GBG ',1, 57.0001030, 12.0001001, 0.1050
408,'HOR ',1, 57.3778000, 12.5583000, 0.3500
409,'RH3 ',1, 57.2588997, 12.1093998, 0.1800
410,'RH4 ',1, 57.2571983, 12.1113997, 0.1800
411,'TRA ',1, 57.4697037, 13.1700001, 0.8000
412,'JKP ',1, 57.6817017, 14.1906004, 0.6600
413,'AVA ',1, 56.8630981, 14.4994001, 0.1500
414,'KHM ',1, 56.3217010, 14.7124996, 0.3000
0 / End of Substation Data, Begin Bus Substation Data
1, 401
2, 402
11, 410
12, 410
91, 409
92, 409
101, 401
103, 403
104, 404
106, 406
107, 407
110, 410
111, 411
112, 412
113, 413
114, 414
205, 405
401, 401
402, 402
403, 403
404, 404
405, 405
406, 406
407, 407
408, 408
409, 409
410, 410
411, 411

412, 412
413, 413
414, 414
0 / End of Bus Substation Data, Begin Transformer Data
401, 1, 0,'1 ', 0.2000, 2.9714, 0.0000,0,0,0,'YND1 ', 4, 0.6600
402, 2, 0,'1 ', 7.5790, 0.1013, 0.0000,0,0,0,'YND1 ', 2, 1.1800
410, 11, 0,'1 ', 0.2840, 0.3475, 0.0000,0,0,0,'YND1 ', 4, 0.6600
410, 12, 0,'1 ', 0.2840, 0.3475, 0.0000,0,0,0,'YND1 ', 4, 0.6600
409, 91, 0,'1 ', 0.2930, 0.3552, 0.0000,0,0,0,'YND1 ', 4, 0.6600
409, 92, 0,'1 ', 0.2935, 0.3536, 0.0000,0,0,0,'YND1 ', 4, 0.6600
401, 101, 0,'1 ', 0.2310, 0.0300, 0.0000,0,0,0,'YNA0 ', 4, 0.6600
403, 103, 0,'1 ', 0.1305, 0.0364, 0.0000,0,0,0,'YNA0 ', 3, 0.2900
404, 104, 0,'1 ', 0.1080, 0.0300, 0.0000,0,0,0,'YNA0 ', 3, 0.2900
406, 106, 0,'1 ', 0.1270, 0.0196, 0.0000,0,0,0,'YNA0 ', 4, 0.6600
407, 107, 0,'1 ', 0.0900, 0.0430, 0.0000,0,0,0,'YNA0 ', 3, 0.2900
410, 110, 0,'1 ', 0.2310, 0.0300, 0.0000,0,0,0,'YNA0 ', 4, 0.6600
411, 111, 0,'1 ', 0.2070, 0.0580, 0.0000,0,0,0,'YNA0 ', 3, 0.2900
412, 112, 0,'1 ', 0.1306, 0.0369, 0.0000,0,0,0,'YNA0 ', 3, 0.2900
413, 113, 0,'1 ', 0.2310, 0.0300, 0.0000,0,0,0,'YNA0 ', 4, 0.6600
414, 114, 0,'1 ', 0.1320, 0.0400, 0.0000,0,0,0,'YNA0 ', 3, 0.2900
405, 205, 0,'1 ', 0.0766, 0.1467, 0.0000,0,0,0,'YNA0 ', 4, 0.6600
0 / End of Transformer Data Q

A.4 GIC Data Output File

```
0 /End of Bus Data, Begin Load Data
401, '>A', 1, , , , , 69.20403, , , 0, 0
402, '>A', 1, , , , , 80.68417, , , 0, 0
410, '>A', 1, , , , , 37.96655, , , 0, 0
410, '>B', 1, , , , , 37.96655, , , 0, 0
409, '>A', 1, , , , , 61.19263, , , 0, 0
409, '>B', 1, , , , , 61.08838, , , 0, 0
401, '>B', 1, , , , , 80.24094, , , 0, 0
403, '>A', 1, , , , , 176.24208, , , 0, 0
404, '>A', 1, , , , , 75.23215, , , 0, 0
406, '>A', 1, , , , , 99.53204, , , 0, 0
407, '>A', 1, , , , , 146.31706, , , 0, 0
410, '>C', 1, , , , , 47.24099, , , 0, 0
411, '>A', 1, , , , , 5.41747, , , 0, 0
412, '>A', 1, , , , , 18.60523, , , 0, 0
413, '>A', 1, , , , , 168.18146, , , 0, 0
414, '>A', 1, , , , , 89.63955, , , 0, 0
405, '>A', 1, , , , , 234.21182, , , 0, 0
0 /End of Load Data
Q /End of GIC Data Changes
```